npj | biofilms and microbiomes

Article

Published in partnership with Nanyang Technological University

https://doi.org/10.1038/s41522-025-00876-7

You are what your fungus eats: diet shapes the microbial garden of a fungus-growing ant

Mariana de Oliveira Barcoto[1] ✉, Raquel Lima de Sousa[1,2], João Gabriel da Silva Soares[3], Rodrigo Henrique dos Santos Garcia[3], Eduardo Ribeiro deAzevedo[3], Lucas William Mendes[4], Odair Correa Bueno[1] & Andre Rodrigues[1] ✉

Fungus-growing ants maintain an ectosymbiotic microbial garden, an intertwined mesh of fungal symbiont hyphae and microbiota growing through plant substrates. Here, we investigate how different plant diets influence the garden lignocellulosic profile, and whether the microbiota respond to dietary changes. Colonies of *Atta sexdens* were provided with four different dietary regimens, varying in fiber composition and nutritional content. Diet changed the garden lignocellulosic profile, also influencing the microbial taxonomic composition. The diet of only leaves enriched the garden in *Bacillus* and *Weissella*, while a diet of only fruits/cereals lead to a *Carnimonas* and *Mesoplasma* enrichment; diets mixing leaves and fruits/cereals intermittently and alternatively enriched the garden in *Bacillus, Mesoplasma*, and *Weissella*. The fungal crop development and the spatial distribution of the microbiota and biofilm also varied according to the diet. Our findings suggest that diet has a pivotal role in determining whether ant colonies function optimally and remain healthy.

Animals eat to obtain the required blend of nutrients for fueling their development and reproduction. As masterly encapsulated by Charles Elton: "Food is the burning question in animal society, and the whole structure and activities of the community are dependent upon questions of food-supply"[1]. Through diet, animals acquire appropriate proportions of amino acids, carbohydrates, fatty acids, sterols, vitamins, minerals, trace elements, and water[2–4]. When an animal forages, it selects, among all the options available in its habitat, foods that supply its nutritional needs, demanding to balance multiple nutrients at once. Foraging, thus, is considered a dynamic process where animals are hypothesized to target key macronutrients (such as protein, carbohydrates, and lipids). Even the microbial community inhabiting the animal gut is thought to influence decisions toward food items[3–7]. Directly or indirectly, the gut microbiota is a key determinant of animals' physiological and ecological processes[8]. By way of illustration, host-microbiota interdependencies have allowed animals to derive energy and nutrients from plant substrates, ultimately influencing animal-plant interactions at community level[9–13].

Through diverse enzymatic and chemical pathways, microbes detoxify metabolites and break down the main plant fiber component: lignocellulose. This is a heteropolymeric, dynamic, three-dimensional matrix made of cellulose, hemicelluloses, and lignin, that give plant cells their structural resistance and high recalcitrance[14,15]. Lignocellulose digestion is usually a teamwork of microbial communities, whose members act in syntrophic and complementary ways[16–18]. When the plant fiber is digested inside the host body (e.g., in the gut or in the rumen), endosymbiotic microbes act most anaerobically to ferment fiber components. This produces primarily short-chain fatty acids, such as acetate, propionate, and butyrate that serve as important energy sources for both the host and its microbiome[9,19–23]. Plant fiber degradation may also occur outside the host body, as is the case of fungus-growing insects (macrotermitine termites, fungus-growing "attine" ants, platypodinae, and scolytinae beetles) and their ectosymbiotic microbial partners. These insects forage for (mostly) plant material, which instead of being eaten, it is used to nourish lignocellulolytic fungi. The fungal symbiont converts, aerobically, plant recalcitrant components into simpler ones. Then the farmer insect eats the fungal crop. Via mycophagy, fungus-growing insects are provided with a nitrogen-enriched diet, that also provides essential vitamins, amino acids, and sterols[9,24–26].

Fungal cultivation by ants is considered an outstanding breakthrough in animal evolution[27]. By outsourcing plant digestion to a fungal symbiont, colonies of leaf-cutting ants belonging to the genus *Atta* (Hymenoptera:

[1]São Paulo State University (UNESP), Institute of Biosciences, Department of General and Applied Biology, Rio Claro, SP, Brazil. [2]University of São Paulo (USP), Faculty of Philosophy, Sciences and Letters at Ribeirão Preto, Department of Biology, Ribeirão Preto, SP, Brazil. [3]University of São Paulo (USP), São Carlos Institute of Physics, São Carlos, SP, Brazil. [4]University of São Paulo (USP), Center for Nuclear Energy in Agriculture, Piracicaba, SP, Brazil.
✉e-mail: m.barcoto@unesp.br; mariana.barcoto@gmail.com; andre.rodrigues@unesp.br

Formicidae: Myrmicinae: Attini: Attina) may function as one of the dominant herbivores in the Neotropics. While one *Atta sexdens* nest may span about 50 m^2 and 8 m deep, foraging up to 1–2 tons of plant material per year, one nest of *Atta cephalotes* may span 2–5 million ants. Such immense structures change soil aeration, pH, CO_2, and nutrient concentrations, making leaf-cutting ants ecosystem engineers[28–34]. *Atta sexdens* colonies, in particular, are one of the most complex and large structures made by animals, comprising around 8000 underground chambers and living up to 20 years[35–37]. Leaf-cutting ant colonies are highly polyphagous, generalist herbivores, which may forage for leaves, flowers, fruits, seeds, twigs, and barks. Within the available substrates, they tend to select young and healthy leaves (though preferring floral parts and fruits when these nutritionally rich items are available) or leaves with increased nutritional content[33,38–41]. Although colonies have a major ecological role as herbivores, leaf-cutting ants themselves are mostly mycophagous. They feed on *Leucocoprinus gongylophorus* (*Basidiomycota*: *Agaricales*: *Agaricaceae*), the fungus they cultivate and from who they obtain most of their carbon and nitrogen inputs[42–45].

Leucocoprinus gongylophorus is a highly domesticated fungal cultivar, nutritionally and morphologically adapted to a symbiotic life with ants[44,46]. Workers inoculate mycelial clumps of *L. gongylophorus* on cut, cleaned, and masticated plant substrates; from cut edges, fungal hyphae spread radially over the substrate. Likely via laccases, glyoxal oxidases, cellulases, hemicellulases, and pectinases, *L. gongylophorus* digests more recalcitrant components to access nutritious plant intracellular contents[42–44,47–51]. The fungus recycles its cellular content through autophagic processes and then concentrates the resulting metabolites in vacuolated cells known as gongylidia[52]. Such cells become swollen as they accumulate essential amino acids, lipids, free sugars, polysaccharides, and plant-degrading enzymes. From the plant substrate, nitrogen, lipids, and cellulose-derived carbon are stored in gongylidia. This nutritious fluid completely nurtures the ant-queen and progeny, and is an important part of workers' diet (adding up to the plant sap workers also consume)[45,52–58]. While growing on a pulped substrate, *L. gongylophorus* forms an intertwined mesh of hyphae, scaffolding a microbiota that colonizes both the hyphae and the plant substrate (Fig. 1A). Apparently adapted to the fungiculture environment, the microbiota is hypothesized to complement the fungal metabolism as it encodes pathways related to lignocellulose degradation, metabolite detoxification, and nutrient biosynthesis. Indeed, some of the bacterial members are reported, in vitro, to fix nitrogen, detoxify plant compounds, solubilize phosphate, form biofilm, and degrade cellulose and chitin[49,59–68].

In leaf-cutting ant microbial gardens the plant decay occurs in a longitudinal continuum, delineating biogeographical regions, and establishing distinct physic-chemical features and microhabitats[51,69–76]. The digestion of freshly added substrates begins with sparse hyphal and microbiota colonization in a gray-green top layer. Hyphae and microbiota density gradually increase as degradation progresses, forming whitish central regions bearing gongylidia clusters (the staphyla). Non-degraded, recalcitrant plant polymers settle at the garden's old parts, structuring a gray-brown bottom region (Fig. 1A, B)[24,48,77–81]. Afterwards, ant workers

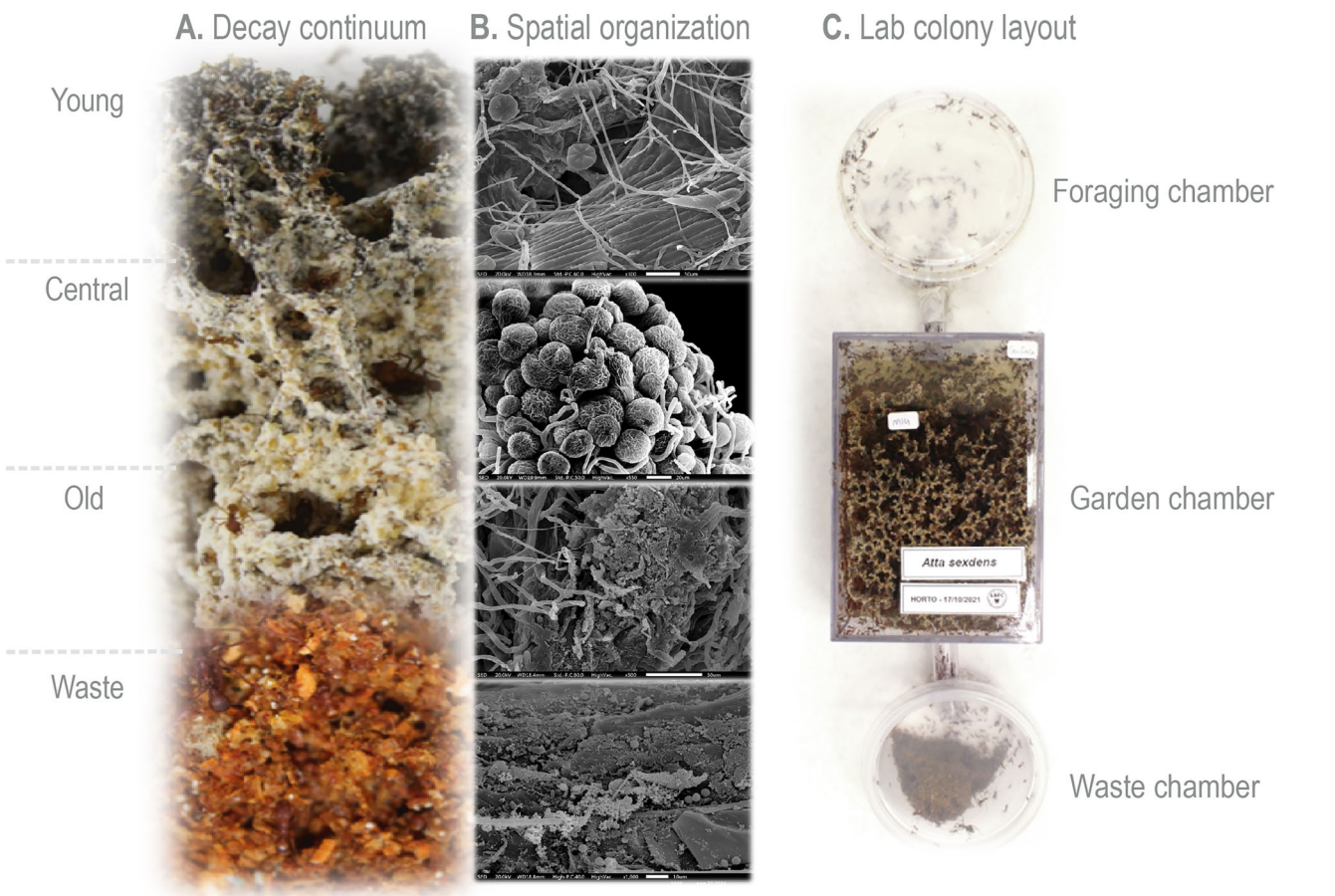

Fig. 1 | Leaf-cutting ant microbial garden. A Substrate gradual digestion delineates the garden young, central, and old regions, as well as the waste, which is removed by ant workers. **B** Scanning electron microscopy detailed the garden spatial organization. Younger regions tend to be sparsely colonized by hyphae, though hyphal abundance increases as substrate degradation progresses, resulting in central regions that are metabolically more active and gongylidia-forming. Older regions present lower hyphae abundance and more degraded substrate. Fragments removed from old regions are separated in waste piles, where the abundant microbiota continues with substrate turnover. **C** We investigated *Atta sexdens* lab colonies, in a set up to provide room for maintaining the garden, the waste, and for foraging.

remove garden portions that have no more nutritional value to waste dumps. Dead workers and harmful substrates are also taken to these dumps, where the abundant microbiota carry on with plant degradation and nutrient cycling, tough not participating in the colony nutrition anymore[60,82–85]. Enzymatic and proteomic data evidenced the leaf-cutting ant garden responding to substrate, in a flexible, fast, and substrate-dependent way[86,87]. However, is yet to be determined whether and to what extent the microbiota take part in the garden metabolic flexibility required to respond to different substrates. Supposedly, the garden microbiota could rapidly adapt to the food content, supporting the garden to cope with seasonal fluctuations in dietary availability[88–93].

The microbial garden is metabolically flexible, expressing a different set of enzymes to respond to recalcitrant and labile substrates[86,87]. Here, we investigate how different plant substrates influence the garden's lignocellulosic profile, and whether the taxonomic composition and spatial distribution of the microbiota respond to these changes. Lab colonies of the leaf-cutting ant *A. sexdens* (Fig. 1C) were subjected to four different dietary regimens over 56 days, varying in fiber composition and nutritional content[94–96]. These diets consisted of: i) Leaves (control group, reflecting the leaf-cutting ants' foraging habits in the field)[32]; ii) Fruits/cereals; iii) Generalist, an intermittent mix of leaves and fruits/cereals; iv) Alternative, which began with leaves, switched to fruits/cereals, and then returned to leaves. We hypothesized that distinct diets would alter the garden chemistry, which in turn would affect the microbiota composition and distribution across garden regions. To test our hypothesis, we first verified the garden's lignocellulosic profile (using ^{13}C Solid-state Nuclear Magnetic Resonance - ^{13}C ssNMR), microbiota taxonomic composition (via metabarcoding), and spatial distribution (using Scanning Electron Microscopy - SEM), along with scoring colony health and functioning. This comprehensive toolkit provided a multidimensional understanding of the microbial garden plasticity and the microbiota's response to environmental fluctuations.

Results

Effects of dietary regimens on lignocellulosic content

The substrates offered to the ants had different lignocellulosic composition, especially regarding the cellulose:hemicelluloses:lignin ratios. Distinct lignocellulose composition, in turn, may create different ecological niches that could favor unique microbial assemblages[51,97–99]. Thus, we attempted to distinguish how different sets of plant substrates could change the garden and waste lignocellulosic profile by ^{13}C ssNMR. Before the experiment began (t_0), colonies of all treatments presented similar general patterns (Fig. 2). Signals in the spectral regions referring to aliphatic compounds (0–50 ppm), derived from lipids and proteins, progressively increased from young garden to waste, supporting biomass degradation, as well as the accumulation of its byproducts, occurring as a continuum.

Overall, signals in the spectral regions related to aromatic rings (110–160 ppm) and methoxy groups (56 ppm) attributed to lignin are still high in the waste, suggesting that lignin is not metabolized in the garden (or at least not completely decomposed). Signals in the spectral regions related to hemicellulose (62, 110, 82 and 173 ppm), on the other hand, are pronouncedly reduced in old regions, and even more in the waste. Thus, hemicellulose seems to be the most degraded (and possibly consumed) biomass component. An estimation of the relative hemicellulose content in the samples can be obtained by analyzing the signal in the 90–110 ppm region. This region is mainly associated with the C1 carbon of carbohydrates, which can generally be resolved into two lines: a broader one at 102 ppm and a narrower one at 105 ppm. This separation is illustrated in the inset on the right side of the top-left panel of Fig. 2, which shows the deconvolution of the signal into these two components. Hemicellulose:cellulose ratio was calculated from the relative areas of the C1 signals at 102 and 105 ppm, and are presented as bar plots. Hemicellulose:cellulose ratio decreases progressively from young to old samples, reaching the lowest values in waste material, indicating a marked depletion of hemicellulose.

During the differential feeding, colonies receiving the Leaves diet did not exhibit substantial variations from the afore described patterns throughout time (Fig. 2A). Conversely, colonies in the Fruits/cereals diet presented a progressive increase in the signal in the spectral region of 100 ppm, conceivably related to hemicellulose accumulation (particularly xylan; Fig. 2B). Colonies receiving the Generalist diet presented increased peaks in the spectral regions of 100 ppm in central and old garden regions after 21 days, in all garden regions after 41 days, and only in old regions after 56 days. This indicates an enhancement in xylan-related hemicelluloses, yet not so conspicuous as in the Fruits/cereals diet (Fig. 2C). While receiving leaves for 20 days, gardens and waste from colonies in the Alternative diet have not evidenced substantial changes relative to the ones in the Leaves diet (Fig. 2D). After receiving fruits/cereals for 20 days, all garden regions began to present increased peaks in the spectral regions of 100 ppm, referring to hemicellulose accumulation (Fig. 2D). Then, when the colonies were returned to leaves for the last 16 days, the increased peaks in the spectral regions of 100 ppm remained only in the old regions of the garden (Fig. 2D). In essence, fruits and cereals lead to an increase in hemicelluloses, particularly the xylan-related ones, throughout the garden regions.

Effects of dietary regimens on the microbiota composition

Bacterial communities were investigated by amplicon sequencing of 16S rRNA genes, yielding 17,538 amplicon sequence variants (ASVs) assigned to Bacteria. Fungal communities were investigated through amplicon sequencing of the ITS region, resulting in 605 ASVs assigned to Fungi. We observed a general pattern in which younger regions were the least rich and diverse, while central and old regions showed similar richness and diversity (Supplementary material, Supplementary Figs. S1–S6). The bacterial phyla *Actinobacteria, Firmicutes* and *Proteobacteria* dominate all garden regions. The waste, far richer and more diverse than the garden, has *Actinobacteria, Bacteroidota*, and *Proteobacteria* as the most abundant bacterial phyla (Fig. 3; Supplementary Fig. S7). In terms of microbiota composition, the bacterial community appears to be more responsive to dietary fluctuations than the fungal community. The fungal community is predominantly dominated by *Agaricaceae* sp. (*Basidiomycota: Agaricales*), likely referring to the fungal crop biomass (Supplementary Figs. S8–S10). By comparing distinct garden regions and diets, we identified: i) Metabolically adaptable microbes, that occur in different garden regions and adapt to distinct diets, such as *Brachybacterium, Glutamicibacter, Methylobacterium*, and the yeast *Haglerozyma*; ii) Leaf-favored microbes, which thrive when the garden receive leaves (recalcitrant substrate), such as the bacterial genera *Achromobacter, Enterococcus, Leucobacter, Paracoccus, and Stenotrophomonas*; iii) Fruit-favored microbes, that flourish when the garden receives fruits and cereals (labile substrate), such as the bacterial genera *Carnimonas* and *Mesoplasma*; iv) Microbes favored by mixed fibers, that prosper when exposed to plant fibers from mixed sources with varying recalcitrance. These include bacterial genera *Advenella, Clostridium, Microbacterium, Paenibacillus, Serratia, Sphingomonas*, and *Streptomyces*, as well as the fungal genera *Escovopsis, Fusarium*, and *Hyphopichia* (Table 1, Supplementary Figs. S11–S18). In summary, there is a spatiotemporal assembly of the microbiota throughout the decay continuum, with each region exhibiting characteristic patterns of richness, abundance, and diversity (Supplementary Figs. S19–S27).

Microbiota of young gardens. In the bacterial community, uncultured *Rhizobiaceae* dominate Leaves, Generalist, and Alternative young gardens throughout 56 days; Fruits/cereals young gardens are otherwise dominated by *Mesoplasma* and *Carnimonas* after 41 days (Fig. 3A). Fruits/cereals young gardens tend to be richer, having higher alpha diversity (Fig. 3B, Supplementary Fig. S20) that differ from Leaves (Wilcoxon test, FDR-adjusted $p = 0.02$), Generalist (Wilcoxon test, FDR-adjusted $p = 0.024$), and Alternative (Wilcoxon test, FDR-adjusted $p = 0.0039$) young gardens. Beta diversity analysis based on Bray-Curtis dissimilarity revealed that the community variation was not significantly correlated with the diet (PERMANOVA, FDR-adjusted $p = 0.162$, Fig. 3C). Uncultured *Rhizobiaceae* explains 32.44 - 44.87% of the dissimilarity

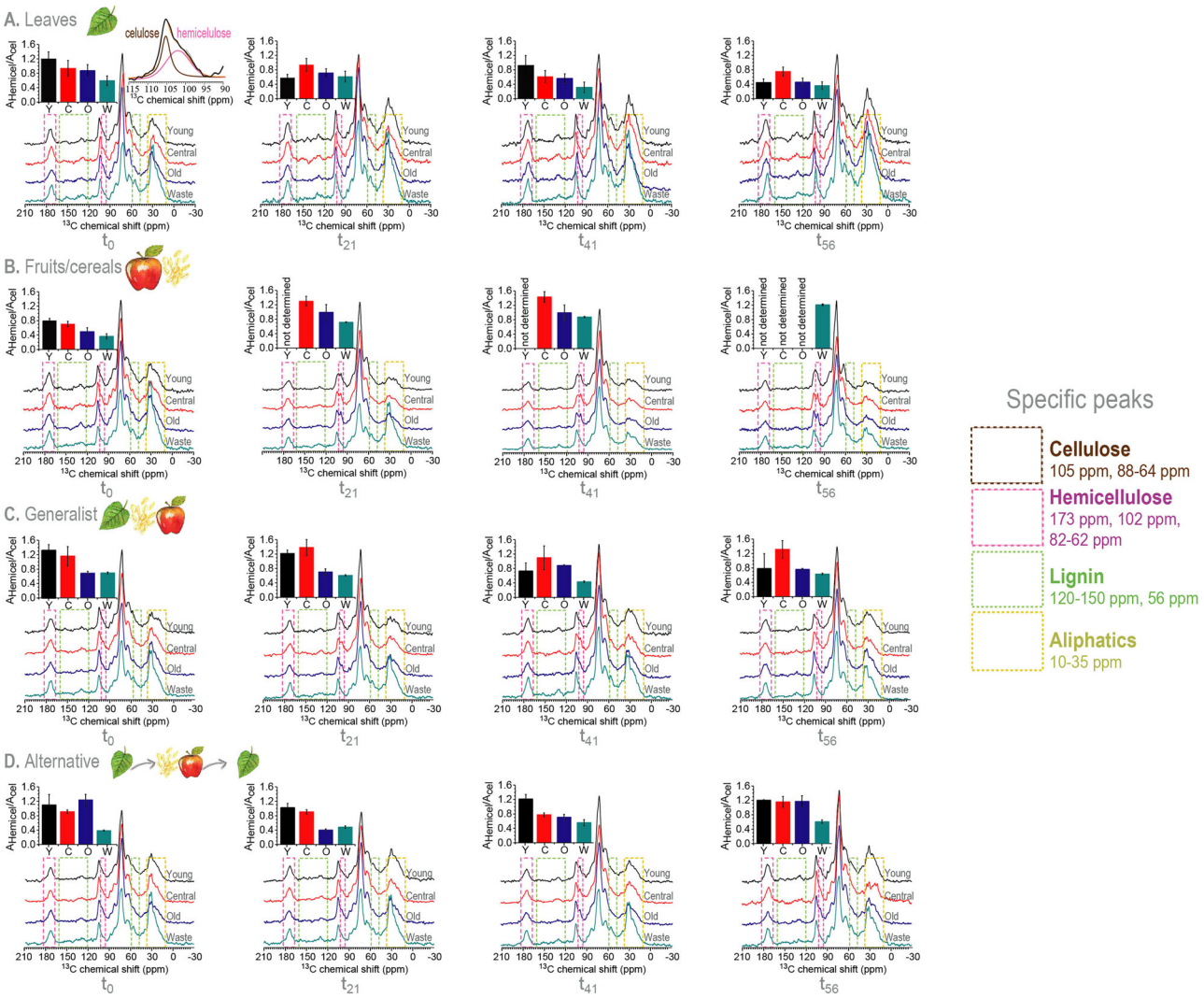

Fig. 2 | Garden lignocellulosic composition in distinct diets. We employed ^{13}C ssNMR to distinguish whether different plant substrates could change the garden and waste lignocellulosic profile. Signals assigned to specific lignocellulose components are shaded in the spectrum. **A** Leaves diet; **B** Fruits/cereals diet; **C** Generalist diet; and **D** Alternative diet. The differential feeding yielded distinct lignocellulosic composition, mainly regarding peaks in the spectral regions of hemicelluloses. The region between 90 and 110 ppm, corresponding to C1 carbons of polysaccharide residues, shows two partially resolved signals: the narrower peak at ~105 ppm, attributed to cellulose microfibrils, and the broader peak at ~102 ppm, attributed to hemicellulose. The inset on the right side of the top-left panel shows the deconvolution of the signal into these two components. Bar plots above each spectrum display the calculated hemicellulose:cellulose ratio based on the relative areas of these two signals. A progressive decrease in this ratio is observed from young to old samples, with the lowest values in waste material, indicating a marked depletion of hemicellulose. Young (Y), central (C), old (O), and waste (W).

between diets (SIMPER, based on Bray-Curtis dissimilarity, Supplementary Material).

In the fungal community, *Basidiomycota* in the family *Agaricaceae* dominated young gardens in most of the samples, regardless of the diet. *Haglerozyma* sp. (*Basidiomycota: Trichosporonaceae*), *Simplicillium* sp. (*Ascomycota: Cordycipitaceae*), and *Escovopsis* sp. (*Ascomycota: Hypocreaceae*) were relatively abundant in Generalist and Leaves young gardens (Supplementary Figs. S8–S10). Generalist young gardens tend to be richer, having slightly higher alpha diversity (Supplementary Fig. S21), though without significant differences between diets (Wilcoxon test, FDR-adjusted $p > 0.05$). Beta diversity analysis based on Bray-Curtis indicates the community variation not being correlated to the diet (PERMANOVA, FDR-adjusted $p = 0.354$, Supplementary Fig. S19), yielding no differences between diet groups (PERMANOVA, FDR-adjusted $p > 0.05$). *Agaricaceae* sp. contributes to 32.86–37.58% of dissimilarity between diets (SIMPER analysis based on Bray–Curtis, Supplementary Material).

Microbiota of central gardens. The bacterial community had uncultured *Rhizobiaceae* initially dominating central gardens receiving all diets. Through time, *Bacillus* increased in Leaves gardens, *Carnimonas* and *Mesoplasma* expanded in Fruits/cereals gardens, and *Mesoplasma* tended to become more abundant in Generalist gardens. In Alternative central gardens, *Mesoplasma* increased in abundance between 21 and 41 days, after which *Bacillus* increased in abundance (Fig. 3A). Leaves and Fruits/cereals central gardens tend to be slightly richer, and alpha diversity differs between Fruits/cereals and Alternative central gardens (Wilcoxon test, FDR-adjusted $p = 0.01$; Fig. 3B; Supplementary Fig S22). Beta diversity analysis based on Bray–Curtis suggests that the community varies according to the diet (PERMANOVA, FDR-adjusted $p = 0.016$, Fig. 3C), with differences between Leaves and Fruits/cereals central gardens (PERMANOVA, FDR-adjusted $p = 0.036$). Taxa contributing to the dissimilarity between diets include uncultured *Rhizobiaceae* (23.08–39.9%), *Bacillus* (2.45–24.78%), *Mesoplasma* (6.9–16.93%), and *Carnimonas* (1.29–11.21%, SIMPER analysis based on Bray–Curtis, Supplementary Material).

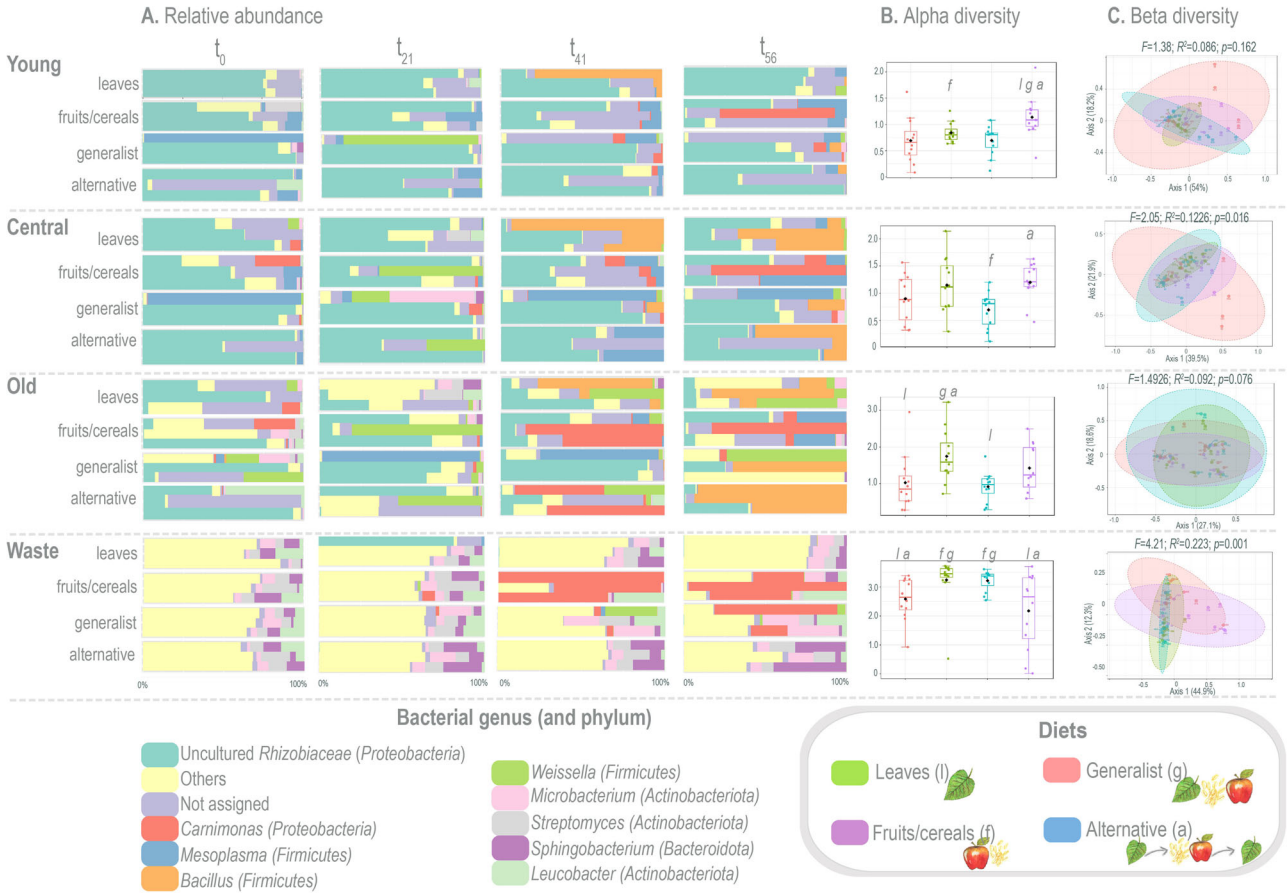

Fig. 3 | Garden microbiota respond to distinct diets. A Relative abundance (%) of bacterial genera (depicting only genera with relative abundance >1%), for the different diets along the experiment. **B** Alpha diversity indices at the genus level based on the Shannon index, estimating significant differences between groups by Mann–Whitney/Kruskal–Wallis, with the Wilcoxon test for post hoc pairwise comparisons (other diversity metrics are presented at the Supplementary Material). Significant differences between diets (Wilcoxon test, FDR-adjusted $p < 0.05$) are indicated by letters (representing the diet that the group differed from - *l:* leaves; *f:* fruits/cereals; *g:* generalist; *a:* alternative). **C** Beta diversity estimated with Principal Coordinates Analysis (PCoA) ordination, based on Bray–Curtis distances; statistical significance of data distribution and pairwise comparisons were defined by PERMANOVA. Both alpha- and beta diversity were calculated based on the total number of genera.

The fungal community had *Agaricaceae* dominating central gardens of all diets (Supplementary Figs. S8–S10). Leaves central gardens tend to be richer, having slightly higher alpha diversity (Supplementary Fig. S23), though without significant differences between diets (Wilcoxon test, FDR-adjusted $p > 0.05$). Beta diversity analysis based on Bray–Curtis indicates the community variation relates to the diet (PERMANOVA, FDR-adjusted $p = 0.041$, Supplementary Fig. S19), yet without differences between diet groups (PERMANOVA, FDR-adjusted $p > 0.05$). *Agaricaceae* sp. explains 35.22–48.73% of dissimilarity between diets (SIMPER analysis based on Bray–Curtis, Supplementary Material).

Microbiota of old gardens. Bacterial community of Leaves old gardens had *Bacillus* and *Weissella* as abundant members, especially after 41 days. *Carnimonas* and *Mesoplasma* dominate Fruits/cereals old gardens from 21 to 56 days. Uncultured *Rhizobiaceae, Bacillus, Mesoplasma*, and *Weissella* oscillate in dominance in Generalist old gardens throughout the experiment. Reflecting the dietary change, *Carnimonas* became abundant in the Alternative old garden after 21 days (after the time when receiving fruits/cereals), then *Bacillus* became abundant after 56 days (after the time when receiving leaves; Fig. 3A). Leaves old gardens tend to be richer, having higher alpha diversity indices (Fig. 3B; Supplementary Fig. S24) that differ from Generalist (Wilcoxon test, FDR-adjusted $p = 0.036$) and Alternative central gardens (Wilcoxon test, FDR-adjusted $p = 0.01$). Beta diversity analysis based on Bray–Curtis suggests that the community variation is not correlated to the diet (PERMANOVA, FDR-adjusted $p = 0.076$, Fig. 3C), reinforced by pairwise comparisons yielding no differences between diet groups. Responsible for dissimilarity between diets are bacterial taxa such as uncultured *Rhizobiaceae* (16.68–24.66%), *Bacillus* (4.02–18.88%), *Carnimonas* (7.65–17.4%), and *Weissella* (8.86–10.6%, SIMPER analysis based on Bray–Curtis, Supplementary Material).

Fungal community of Leaves and Alternative old gardens had *Haglerozyma* sp. and *Escovopsis* sp. as abundant members, and the abundance of *Fusarium* sp. (*Ascomycota: Nectriaceae*) was slightly higher in Leaves old gardens. *Agaricaceae* sp. dominated Generalist old gardens, and *Hyphopichia* sp. (*Ascomycota: Saccharomycetales*) increased in abundance in Alternative and Fruits/cereals old gardens (Supplementary Figs. S8–S10). Leaves old gardens are slightly richer, closely followed by Alternative and Fruits/cereals old gardens, while Alternative old gardens have higher alpha diversity (Supplementary Fig. S25), which differs from Generalist old gardens (Wilcoxon test, FDR-adjusted $p = 0.041$). Beta diversity analysis based on Bray–Curtis suggests the community variation does not relate to the diet (PERMANOVA, FDR-adjusted $p = 0.342$, Supplementary Fig. S19), with differences between Generalist and Alternative old gardens (PERMANOVA, FDR-adjusted $p = 0.036$). *Agaricaceae* sp. is responsible for 26.57–34.57% of dissimilarity between diets (SIMPER analysis based on Bray-Curtis, Supplementary Material).

Waste microbiota. Bacterial community of Leaves, Generalist, and Alternative waste is mostly (between 25 and 50%) assigned as "others"

Table 1 | Bacterial genera differentially abundant in diet groups and garden sites, as determined by heat tree analysis[231] comparing group-wise relative abundances (Wilcoxon test, $p < 0.05$)

	Leaves diet	Fruits/cereals diet	Generalist diet	Alternative diet
Young gardens	*Antricoccus* [f] *Bacillus* *Bogoriella* *Glutamicibacter* [f] *Mesoplasma* [f, a] *Ochrobactrum* *Patulibacter* [f]	*Antricoccus* [l] *Amaricoccus* *Aeromicrobium* *Brevundimonas* *Carnimonas* [g] *Glutamicibacter* [l] *Mesoplasma* [l, a] *Methylobacterium* [g] *Parapusillimonas* *Parapedobacter* *Patulibacter* [l] *Paenibacillus* [g] *Pelagibacterium* *Sphingopyxis* *Staphylococcus* [g, a]	*Advenella* *Carnimonas* [f] *Cutibacterium* [a] *Methylobacterium* [f] *Paenibacillus* [f] *Staphylococcus* [f, a]	*Mesoplasma* [l, f] *Cutibacterium* [g] *Staphylococcus* [f, g]
Central gardens	*Achromobacter* *Aureimonas* [g] *Bacillus* [g, a] *Bogoriella* *Brachybacterium* [g,a] *Enterococcus* *Methylobacterium* *Nocardioides* *Parapedobacter* [g] *Pelagibacterium* *Phenylobacterium* [g] *Pseudactinotalea* *Sphingobacterium* [f, g]	*Carnimonas* [g] *Mesoplasma* *Mordicisalibacter* *Sphingobacterium* [l, g]	*Aureimonas* [l] *Arachidicoccus* *Bacillus* [l, a] *Brachybacterium* [l, a] *Brevundimonas* *Carnimonas* [f] *Gordonia* *Kocuria* *Massilia* *Microbacterium* *Parapedobacter*[l] *Phenylobacterium* [l] *Olivibacter* *Sphingobacterium* [l, f] *Sphingomonas* *Streptomyces* *Weissella*	*Acinetobacter* *Bacillus* [l, g] *Brachybacterium* [l, g]
Old gardens	*Achromobacter* *Aeromicrobium* *Antricoccus* [f] *Bosea* *Brachybacterium* *Glutamicibacter* [f] *Leucobacter* *Mesorhizobium* *Nocardioides* *Ochrobactrum* [f] *Paracoccus* *Patulibacter* *Pelagibacterium* [f] *Pseudomonas* *Serratia* *Spelaeicoccus* *Stenotrophomonas*	*Antricoccus* [l] *Carnimonas* *Glutamicibacter* [l] *Mesoplasma* *Modicisalibacter* *Novosphingobium* *Ochrobactrum* [l] *Pelagibacterium* [l]	*Acinetobacter* *Clostridium* *Flavobacterium* *Ligilactobacillus*	*Alterythobacter* *Akkermansia* *Parapusillimonas*
Waste	*Acinetobacter* [g] *Aeromicrobium* *Alterytrhobacter* *Antricoccus* *Bacillus* *Bogoriella* *Brevundimonas* *Camelimonas* *Devosia* [a] *Enterococcus* *Hephaestia* *Luteimonas* *Nocardioides* Novosphingobium Ottowia Pseudochrobactrum *Pusillimonas* *Vagococcus* *Verticiella*	*Carnimonas* [g] *Luteibacter* *Niabella* [a] *Pseudactinotalea* [a]	*Acinetobacter* [l] *Carnimonas* [f] *Floricoccus* *Ochrobactrum* [a] *Serratia* *Streptomyces* *Weissella*	*Achromobacter* *Bordetella* *Bosea* *Daeguia* *Devosia* [l] *Labrys* *Luteibacter* *Microbacterium* *Moheibacter* *Niabella* [f] *Ochrobactrum* [g] *Olivibacter* *Parapusillimonas* *Pseudactinotalea* [f] *Pseudomonas* *Pseudoxhantomonas* *Reyranella* *Shinella*

Some abundant genera are shared between diets (indicated by letters representing the diet which the genera are shared with *l* leaves, *f* fruits/cereals, *g* generalist, *a* alternative), while some tend to be abundant in one diet or another (Supplementary Figs. S11–S18).

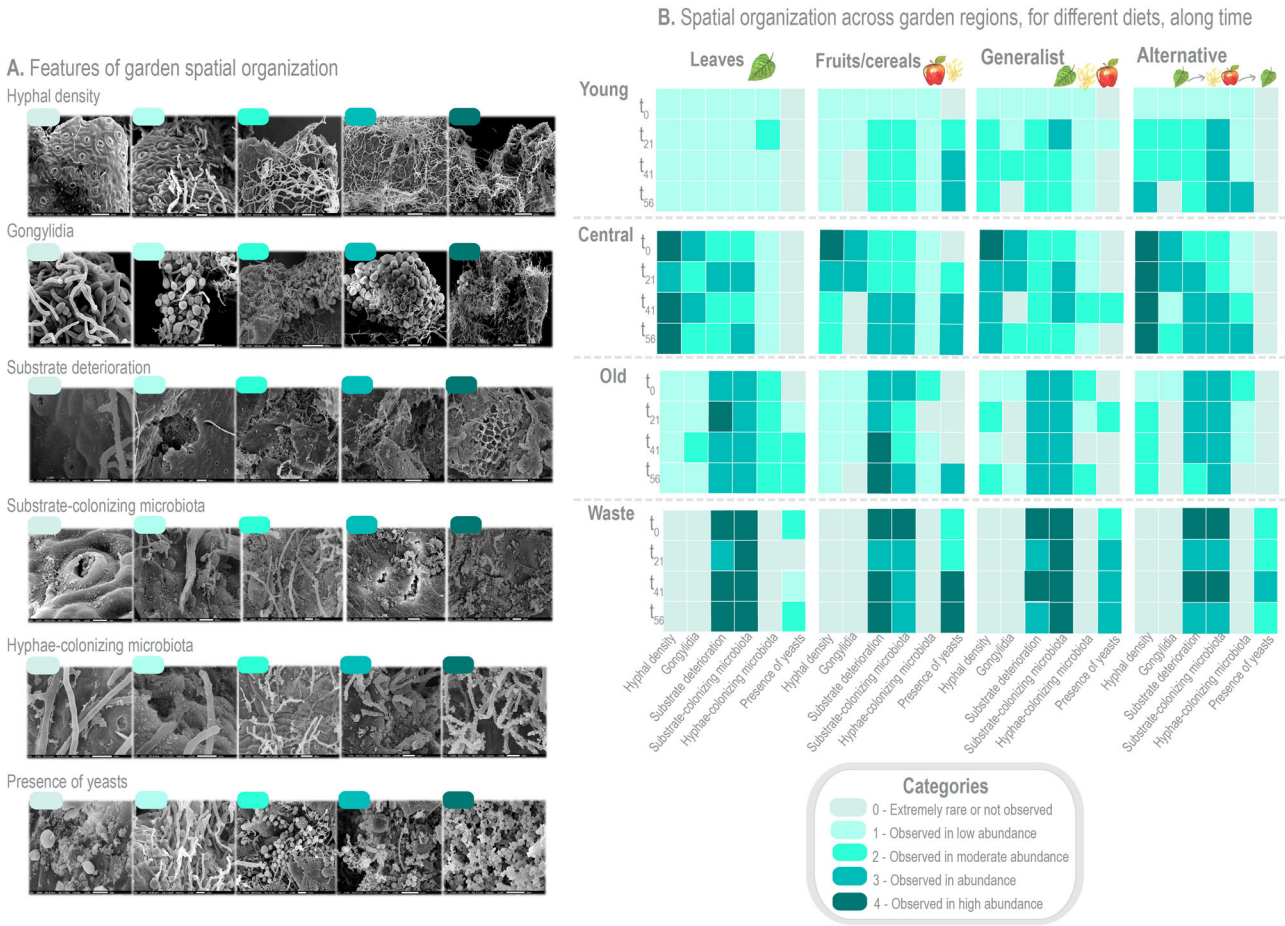

Fig. 4 | Garden spatial distribution in response to diet. A Characterization of garden features observed by SEM imaging along the experiment: hyphal density, presence of gongylidia, signs of substrate deterioration, substrate-colonizing microbiota (including spread biofilms and 3D biofilms, as defined by Barcoto et al.[65]), hyphae-colonizing microbiota, and presence of yeasts. **B** Each feature was categorized as 0 to 4, from rare to high abundance. Features and the frequency they were observed in SEM analysis were gathered as heatmaps for each garden region.

(i.e., genera with abundance <1%); *Leucobacter, Microbacterium, Sphingobacterium*, and *Streptomyces* are also abundant. These genera were abundant for up to 41 days in Generalist waste, from when *Carnimonas* also become abundant. From 21 to 56 days, *Carnimonas* dominated the Fruits/cereals waste (Fig. 3A). Leaves and Alternative wastes are richer and have higher alpha diversity indices (Fig. 3B; Supplementary Fig. S26). These differ from Fruits/cereals waste (Wilcoxon test, FDR-adjusted $p = 0.006$), Generalist (Wilcoxon test, FDR-adjusted $p = 0.003$), and Alternative waste (Wilcoxon test, FDR-adjusted $p = 0.01$). Alpha diversity in Alternative wastes differs from both Generalist (Wilcoxon test, FDR-adjusted $p = 0.003$) and Fruits/cereals (Wilcoxon test, FDR-adjusted $p = 0.006$). Beta diversity analysis based on Bray-Curtis denotes the community variation being correlated to the diet (PERMANOVA, FDR-adjusted $p = 0.001$, Fig. 3C), reinforced by pairwise comparisons yielding differences between almost all diet groups. Dissimilarity between diets is mainly explained by *Carnimonas* (6.55–25.19%) and *Microbacterium* (2.95–11.33%, SIMPER analysis based on Bray-Curtis, Supplementary Material).

The fungal community contrasts to other garden regions once *Ascomycota* is more abundant than *Basidiomycota*. Although *Haglerozyma* sp. is most prevalent in the Alternative waste, it is abundant in waste samples across all diets. *Fusarium* sp. is abundant in both Leaves and Alternative wastes, while *Acremonium* sp. (*Ascomycota: Bionectriaceae*) is more prominent in Alternative and Fruits/cereals (Supplementary Figs. S8–S10). Although alternative waste is richer, waste from all diets have similar alpha diversity indices (Supplementary Fig. S27) with no significant differences between (Wilcoxon test, FDR-adjusted $p > 0.05$). Beta diversity analysis based on Bray-Curtis dissimilarity suggests that the community varies according to the diet (PERMANOVA, FDR-adjusted $p = 0.001$, Supplementary Fig. S19), with all diets differing from each other (PERMANOVA, FDR-adjusted $p < 0.05$). Dissimilarity between diets is mainly explained by *Arthrographis* sp. (6.18–28.25%), *Haglerozyma* sp. (10.66–26.32%), and *Hyphopichia* sp. (0.12–12.38%, SIMPER analysis based on Bray–Curtis, Supplementary Material).

Microbiota changes its spatial distribution in response to diet, especially by forming biofilm

Not only the taxonomic composition but also the microbiota spatial distribution changed according to the diet. We employed SEM for describing garden and waste microstructure, as well as microbiota-substrate and microbiota-hyphae physical interactions, at four time points: before the experiment (t_0), after 20 days (t_{21}), after 40 days (t_{41}), and after 56 days (t_{56}). By visually analyzing the resulting 930 SEM images, we verified the response to different diets including changes in garden spatial organization and microbiota distribution (Fig. 4A).

Before the experiment (t_0), substrate deterioration, hyphal density, microbiota colonization, and biofilm complexity tended to gradually increase from young to old regions, for all diet groups. Hence, young, less deteriorated regions, were sparsely colonized by hyphae and microbiota, which grow at foliar surfaces, isolated or as small communities. In the central parts, hyphal density increases, and clusters of gongylidia become more abundant, both being often surrounded by biofilms of varied structure. Old

Fig. 5 | Colony health and functioning when receiving four different diets. Colonies health and functioning were evaluated according to a standard score scale (Table 2). **A** Acceptance, **B** garden health conditions, **C** substrate decay continuum, and **D** waste were scored for Leaves diet, Fruits/cereals diet, Generalist diet, and Alternative diet. Markers represent the score media and the standard variation for each day. Significant differences between diets (Friedman's two-way ANOVA by ranks post hoc test, $p < 0.05$) occurred only at the days appearing in the x-axis of the graphs, which were colored according to the group(s) they differed from. Comparisons between test groups are available as Supplementary Material.

regions are characterized by lower hyphal density (often surrounded by biofilm), besides deteriorated substrate hosting a dense microbiota in its furrows and indentations. Substrates observed in the waste are extensively deteriorated, inhabited by 3D multi-morphological biofilms and yeasts, seemingly interacting physically.

Such distribution patterns did not change at the three remaining time points for Leaves gardens (Fig. 4B). Fruits/cereals gardens markedly lost the typical distribution patterns after t_{21}, with the hyphal density decreasing in parallel to a marked increase in microbiota colonization and the presence of yeasts, in all garden regions (Fig. 4B). Patterns observed in Generalist gardens presented intermediate features between Leaves and the Fruits/cereals gardens, not varying perceptively from t_0 up to t_{56}. In central regions, we observed the most discernible feature of this group: lower hyphal density, without discernible staphyla or yeasts (Fig. 4B). Alternative gardens presented similar patterns to Leaves gardens at t_{21}, after which we observed a reduction in hyphal density and an increase in biofilm over the substrate and hyphae. At t_{41}, there was an expansion in the yeast community in central and old regions, though not as outstanding as in Fruits/cereals gardens. At t_{56}, gardens presented biofilms colonizing the hyphae surface, yet exhibiting gongylidia once again (Fig. 4B). In summary, the garden spatial organization goes through a reconfiguration when fruits and cereals are given to the colonies, as hyphal density and the presence of gongylidia tend to decrease. This occurs either when fruits are the sole resource, an intermittent resource, or an alternative resource. Besides, in response to fruits and cereals in the diet, the microbiota colonizing substrate and hyphae seem to expand, mostly in the form of spread and 3D biofilms.

Diet impacts colony health and functioning

Health and functioning of the colonies were assessed by scoring the substrate acceptance, the garden health conditions, maintenance of the decay continuum, and waste aspects (Fig. 5). Leaves, Generalist, and Alternative diets were, in general, well accepted and incorporated throughout the experiment, and did not significantly differ among them (Friedman's two-way ANOVA by ranks post hoc test, $p > 0.05$; Fig. 5A). The Fruits/cereals diet was well accepted up to the tenth day, after which the acceptance oscillated, tending to decline, significantly differing from the other diets in several days (Friedman's two-way ANOVA by ranks post hoc test, $p < 0.05$; Fig. 5A). Garden health conditions of colonies receiving Leaves and Alternative diets oscillated, though the colony functioning remained stable. Although the garden health conditions decreased when colonies of the Alternative diet received the "fruits/cereals" treatment, they significantly differed from the Leaves diet only at day 38 (Friedman's two-way ANOVA by ranks post hoc test, $p < 0.05$; Fig. 5B). Some oscillation tending to decline was observed in garden health of colonies receiving the Generalist diet, although they did not significantly differ from colonies that received Leaves and Alternative diets (Friedman's two-way ANOVA by ranks post hoc test, $p > 0.05$). Even though the garden health of colonies receiving the Fruits/cereals diet differed from Leaves and Alternative in several periods, they declined the most at the last four days of the experiment (Friedman's two-way ANOVA by ranks post hoc test, $p < 0.05$; Fig. 5B).

The longitudinal decay continuum was kept in colonies fed with Leaves and Generalist diets, while virtually disappeared in colonies that received Fruits/cereals diet, differing from the other diets from day six to the end of the experiment (Friedman's two-way ANOVA by ranks post hoc test, $p < 0.05$). Colonies in the Alternative regimen partially lost their decay continuum during the time they were given the "fruits/cereals" alternative, a period in which they differed from Leaves diet (Friedman's two-way ANOVA by ranks post hoc test, $p < 0.05$; Fig. 5C). Waste parameters oscillated coincidently with the sampling time, and the test groups differed punctually between them (Friedman's two-way ANOVA by ranks post hoc test, $p < 0.05$; Fig. 5D). Briefly, the Fruits/cereals diet negatively influenced the acceptance, garden health, and the decay continuum. This was also observed in the Alternative diet when the colonies were feed with fruits and cereals (between t_{21} and t_{41}).

Discussion

Metabolic plasticity of host-associated microbiota is key for animals to cope with energetic challenges imposed by seasonal oscillations in resource

availability. Such buffering mechanisms were already reported for wild herbivores when feeding on distinct plant organs as these were available throughout the seasons[88–93]. Distinct plant organs differ in nutrient composition, as a consequence of being made of several cell types *per* the role they play in the plant development. Each plant cell is surrounded by a dynamic matrix of several polysaccharides, grouped under the umbrella term "plant fiber"[100,101]. To be digested, plant fiber requires to encounter microbes that express an enzymatic arsenal able to break down its precise set of chemical linkages, as well as to metabolize the resulting byproducts. To be nourished by plant fiber, microorganisms need, beyond enzymes, to be able to stick to the substrate (e.g., by forming biofilm) and tolerate the environmental changes (e.g., due to acidity and osmolarity) as fiber is broken apart[101–103]. Thus, we conceive the longitudinal decay continuum that composes the leaf-cutting microbial garden (Fig. 1) as a spectrum of microhabitats, rendering a multitude of microbial niches derived from fiber decomposition[102]. Distinct plant substrates received as different dietary regimens shaped such microhabitats, affecting the garden in several interconnected dimensions: the garden lignocellulosic profile, the microbiota spatial distribution and composition, and the colony health.

Leaves, fruits, and cereals fibers differ in monosaccharide composition, glycosidic bonds (whose distinct patterns may create either linear or branched structures), and polymerization degree, thus having distinct physicochemical properties[94,95,101,104]. At last, each diet represented particular combinations of fiber types, yielding gardens with different lignocellulosic profiles (Fig. 2). Before the differential diets, ^{13}C ssNMR revealed all colonies characterized by a continuum of lignocellulose decay from young garden regions to the waste, in parallel with lipids and protein accumulation. Agreeing with enzymatic and proteomic data[48,79,80,105–108], hemicellulose was degraded to a vast extent throughout the decay continuum, and lignin was not completely broken down (Fig. 2). Whether leaves-derived fibers (as the sole fiber source) did not change the garden characteristic decay continuum, fruits- and cereals-derived fibers did quite the opposite. When fruits and cereals were the sole fiber source (Fruits/cereals diet), they enriched all garden regions and the waste with hemicelluloses, especially xylan. When provided intermittently (Generalist diet) or in an alternate way (Alternative diet), fruits- and cereals-derived fibers increased hemicelluloses in all garden regions, though more prominently at young and central parts. Fruits- and cereals-derived fibers indeed enriched the garden in hemicellulose, since as soon as leaves became the sole source of plant fiber, gardens from the Alternative diet recovered the characteristic decay continuum (Fig. 2D). Distinct fiber pools in the form of different diets provide a variable set of spatial and nutritional niches, shaping the microbiota time-dependently (Figs. 3 and 4)[101,109,110]. No known microorganism is able to handle the breakdown of all plant polysaccharides; each species, instead, targets only a portion, a discrete structure of the entire fiber content. Then, microbial species interact in intertwined food chains where species overlap their partial fiber-degrading capacity, by means of syntrophic cross-feeding and/or competitive strategies[96,111]. These end up determining fiber digestibility, regulating which nutrients are released from the plant tissue, and ultimately, establishing microbial-environment interactions[100,112].

Lignocellulose-derived gradient (Fig. 2) yields variable microhabitats or spatial niches to be colonized by particular community members[113]. This stratifies the microbiota, setting a gradual increase in microbial richness, abundance, and diversity (Fig. 3; Supplementary Figs. S1–S6). The taxonomic composition also follows the continuum: whereas the microbiota of young, central, and old regions resides mostly in the bacterial phylum *Proteobacteria, Actinobacteria*, and *Firmicutes*, the latter is replaced by *Bacteroidota* in the Waste (Supplementary Fig. S7). Something similar happens in the fungal realm, once the *Basidiomycota* dominance in all garden regions is replaced by the *Ascomycota* dominance in the waste (Supplementary Figs. S8–S10). Changing the diet, then, changes the bacterial genera composition: the leaves diet tended to enrich the garden in *Bacillus* and *Weissella;* fruits/cereals diet lead to a *Carnimonas* and *Mesoplasma* enrichment; and the diets mixing leaves and fruits/cereals intermittently and alternatively enriched the garden in *Bacillus, Mesoplasma*, and *Weissella*. The nature of our sequencing data does not allow to access the metabolic potential of these bacterial genera. Even when suggesting their putative role in the garden based on the literature, the scenario where they are transient components of the microbiota should also be considered. It is important to mention that our study lacks environmental controls (i.e., blank controls), which raises the possibility of: i) cross-contamination between samples and environment (including reagents, laboratory surfaces, or human operators); ii) contaminant DNA reducing the representativeness of low-abundance taxa; and iii) transient microbes (temporary members of the microbiota) and relic DNA (genetic remains of dead cells) influencing ecological interpretations[114,115]. For this reason, we avoided conjecturing too extensively on the potential role of the microbial genera for the garden ecology, focusing on pattern changes.

In colonies receiving Leaves and Alternative diets, *Bacillus* and *Weissella* strains could rely on their lignocellulolytic potential to digest leaves' fibers, as they do so in leaf-litter, cow dung, and spontaneous food fermentation processes[116–121]. *Carnimonas* and *Mesoplasma* are bacterial genera that may be associated with sugar-enriched environments, such as the gut of phloem sap-sucking psyllid *Leptynoptera sulfurea*[122], the guts of solitary bees *Megachile sculpturalis* and *Anthidium florentinum*[123], as well as in the bee bread of honey and stingless bees[124–128]. In colonies receiving fruits and cereals, *Carnimonas* and *Mesoplasma* could engage in pathways for metabolizing the simpler carbohydrates accumulated in the garden.

Besides these abundant genera, others were revealed to thrive in one or other diet (Table 1), though not being clear what paved their adaptation neither their putative role in the colonies. Metabolically adaptable microbes occur in different garden regions, in distinct diets, and possible adapt to the garden changes according to the diet. Among these genera, there are diazotrophs (e.g., in the genera *Brachybacterium*[129]), denitrifiers and fungal-growth promoters (e.g., in the genera *Glutamicibacter*[130,131]). Leaf-favored microbes include genera that are members of the phyllosphere (e.g., *Aeromicrobium, Leucobacter, Nocardioides*)[132,133], and rhizosphere (e.g., *Paracoccus*[134] and *Stenotrophomonas*[135]), being frequently associated with plants[136]. There is also a wide group of microbes, of diverse ecology and lifestyles, that appear to prosper when finding mix of plant fibers, from labile to recalcitrant, originated from leaves, fruits, and cereals, like in the Generalist and Alternative diets. These include genera described as lignocellulolytic and fiber-degrading aerobes (e.g., *Advenella*[137], *Microbacterium*[138,139], *Paenibacillus*[140,141], *Serratia*[142], *Streptomyces*[143,144]) and anaerobes (e.g., *Akkermansia*[145] and *Clostridium*[146,147], although both genera may tolerate oxygen to some extent[148,149]). The fungal genera *Escovopsis, Fusarium*, and *Hyphopichia*, already reported in leaf-cutting ants gardens, are also favored by mixed fibers (Supplementary Figs S11–S18)[150–156].

Fruits and cereals, either being the sole, an intermittent, or an alternative resource altered the fungal crop development and the microbiota architecture. *Leucocoprinus gongylophorus* hyphae reduced in density and ceased gongylidia production. Substrate- and hyphae- colonizing microbiota became wider, mainly as spread and 3D biofilms (Fig. 4B). We presume the high free sugar content in dried fruits changes the garden nutritional profile, enriching it in labile carbon forms such as fructose, glucose, sucrose, and maltose[157,158]. Concurrent events could then emerge: i) catabolic repression of the fungal crop, ii) biofilm expansion, iii) reconfiguration of microbiota composition and dynamics. These possibilities could sum up, resulting in distinct microbial landscapes deriving from fruits as a constitutive garden resource. Simple saccharides, such as glucose, saccharose, and xylose, act as transcriptional regulators that repress or promote the expression of lignocellulolytic enzymes in some filamentous fungi[158–160]. *Leucocoprinus gongylophorus* catabolism of plant components could be, supposedly, repressed by glucose, cellobiose, or xylose[158,159], having its growth impaired by higher sugar concentrations[161,162]. Since glucose and xylose also repress the expression of hemicellulases[159], non-consumed hemicelluloses could have accumulated throughout the garden (Fig. 2). Glucose, fructose, sucrose, and non-resistant starch may also induce cells to aggregate in biofilms, within which bacterial cells grow faster, rendering

larger microcolonies. Biofilm spatial organization and 3D architecture vary according to saccharides concentrations and combinations[163–165]. Although nutrient-rich, dried fruits have low water activity (a_w), which could favor microbial taxa able to thrive in a sugary environment (copiotrophs, i.e., fast-growing microbes), while disfavoring those unable to deal with such physicochemical properties (oligotrophs, i.e., slow-growing microbes)[157,166]. This could contribute to the changes in the garden microbial composition, diversity (Fig. 3), and spatial organization (Fig. 4), and ultimately, redefine microbial interactions[166–170].

A diet based on fruits and cereals pronouncedly impacted colonies functioning, decreasing substrate acceptance, garden health, and the decay continuum. Substrate acceptance was reduced after ten days, suggesting that at this meantime, fruits and cereals could gradually induce garden responses detectable by the ants (Fig. 5). Several findings indicate that garden-ant communication could be fine-tuned at nutritional and molecular levels. For instance, attine workers seem to forage for substrates matching the fungal crop nutritional requirements, with that maintaining the protein:carbohydrate ratio that optimizes hyphal growth[171,172]. Further, while substrates unpalatable to the ants trigger substrate rejection at the foraging site, palatable substrates that harm the garden are rejected with a delay: it requires the garden to respond to the substrate and the ants to identify the response[82,173–178]. Ants also detect metabolic cues of fungal infection over the garden[179], and pick out between linolenic acids[57], therefore it seems plausible that other metabolic changes in the garden could be discerned as well[178]. Changes in metabolites could be a byproduct of the lignocellulosic profile becoming enriched in xylan-related hemicelluloses (Fig. 2), altering the protein:carbohydrate ratio. Non-mutually exclusively, recognizable metabolite changes could derive from recasting the microbiota composition in response to such newly open niches[180,181] (Figs. 3 and 4), or yet, novel fungal-microbiota interactions triggered by such changes[182]. Since there seems to be an association between microbial spatial disturbance (e.g., by biofilm expansion) and decrease in colony health, we expect microbial interactions being altered in the course of diet changing[183,184]. Future integrative research coupling multi-omics[185–187], 3-D imaging[188–194], and chemical ecology[51,194–197] could unveil whether, when, and where these interactions occur, and how impactful these networks are for the microbial garden physiology[198,199].

The microbiota responds fast and flexibly to the variable food content, yet it may be maladaptive for the host: depending on the extent to which the microbiota is reshaped and on the functional outcome of the recasting, dysbiotic states may be induced[200–203]. Dysbiosis refers to compositional changes in the microbiota paralleling functional changes or even loss of physiological features. Microbiota reconfiguration and its altered dynamics may end in loss of beneficial or key microorganisms for the ecosystem functioning, expansion of potential pathogens, and loss of microbiota taxonomic and functional diversity[200,204]. All these possibilities could sum up into microbiota malfunctioning and ecosystemic collapse[205]. Changing the diet of *A. sexdens* lab colonies resulted in distinct lignocellulosic composition of the garden, associated with changes in microbiota composition and spatial distribution. Fruits and cereals, in particular, altered the microbiota composition and architecture, as well as the fungal crop development. We are far from fully understanding the microbial dynamics in the garden, thus far from defining how are the microbial interactions in a healthy garden, or in a diseased one[206]. Though, as the microbiota recasting overlaps with colonies' impaired health and functioning, we suggest the Fruits/cereals diet as inducing dysbiosis in *A. sexdens* colonies. Microbial gardens are responsive to dietary changes as the microbiota of humans[207,208], corals[209,210], cnidarians[211], mice[169,212], and goats[203], that become dysbiotic when facing substantial alteration in the nutritional landscape. Such changes disturb fine-tuned microbial interactions, so much so that ecosystemic dynamics become dysfunctional[207,213]. Our findings suggest a connection between the microbial response to nutritional fluctuations and the colony physiology. Still keeping in mind the lab scale of our experiments, the microbial garden going through a dysbiotic state due to dietary changes raises questions on ant-microbiota interactions: Whether the ants have substrate choice as they have in nature, would dysbiosis occur yet? Could the ants be able to detect and/or counteract dysbiosis? Does dysbiosis play any role in the substrate delayed rejection, or even in substrate selection by the ants? Could the ants learn from the healthy microbiota or from dysbiosis cues? These questions are beyond the scope of the present study, but could be pursued to holistically integrate the ants, their memory and learning[177,214] to the microbial processes occurring in the microbial garden. Our findings emphasize how extensively the diet may shape the microbiota: it defines the nutritional landscape, the microbiota composition and its spatial distribution, ultimately determining whether *A. sexdens* colonies function properly and healthily or not. These findings accentuate the relevance of coupling techniques for a multidimensional understanding of microbiota dynamics, also emphasizing how valuable the microbial garden is as a study model with so much to teach.

Fungus-growing *A. sexdens* ants build massive colonies, which have a major ecological role as generalist and polyphagous herbivores. Their fungal crop, plant substrate, and microbiota join together to form the microbial garden, characterized by a decay continuum along which distinct lignocellulosic contents are established. This assembles the microbiota across space and time, setting a gradual increase in microbial richness, abundance, and diversity. Here, we show that different plant substrates define the garden lignocellulosic profile, with the microbiota spatial taxonomic composition and distribution responding to these changes. Each diet seemed to favor a group of microbial members, evidencing that the microbiota is a constituent part of the garden responses. The diet composed exclusively of fruits and cereals was the most impactful, negatively influencing the acceptance, garden health, and the decay continuum. It increases the hemicellulose content, particularly the xylan-related ones, throughout the garden regions. The garden spatial organization goes through a reconfiguration, as hyphal density and presence of gongylidia tend to decrease. Not only the microbiota taxonomic composition changes, but its distribution in the garden also does so. Such alterations derived from a diet composed of fruits and cereals were vast enough to induce dysbiosis in the microbial garden. Our study provided a multidimensional comprehension of the microbial garden dynamics, associating it with the colony physiology.

Methods

Colonies maintenance and diet formulation

Atta sexdens colonies were collected in the summer of 2021 at the Floresta Estadual Edmundo Navarro de Andrade, Rio Claro, São Paulo State, Brazil (-22°24'43.7580", -47°32'16.7604"). Colonies containing the garden, the queen, workers and offspring were reared until reaching two years old, by the Laboratory of Leaf-cutting Ants (LAFC, UNESP, Rio Claro). Colonies were kept at ~24 °C and 70% relative humidity, with a daylight regime (12 h:12 h light-dark cycle), in a three-set layout to provide room for maintaining the garden, the waste, and for foraging (Fig. 1C). The garden is kept in a plaster-layered central chamber (acrylic container with 16.5 cm length × 11 cm width × 7 cm height, that allows the garden reaching up to 1000 cm^3), with plaster for balancing garden moisture. The central chamber is connected by plastic tubes to the waste and foraging chambers (350 mL polypropylene containers)[215]. Plant substrates were selected according to the literature[33,39,40,215–218]. Previous to the experiment, colonies were acclimated for 30 days, in each day receiving one of the following plant substrates *ad libitum*: dry leaves of orange (*Citrus sinensis*) and eucalyptus (*Eucalyptus globulus* and *Eucalyptus cinerea*), dry and fresh leaves of mulberry (*Morus nigra*), dry flowers of *Hibiscus rosa-sinensis*, and also fresh leaves of *Hibiscus* sp., mango (*Mangifera* sp.), and jambolan (*Syzygium cumini*). Cereals such as oat flakes (*Avena sativa*) and rice grains (*Oryza sativa*), and dehydrated fruits such as apple (*Malus domestica*), papaya (*Carica papaya*), mango (*Mangifera indica*), banana (*Musa* spp.), and guava (*Psidium guajava*). During this period, we recorded which substrates were better accepted, as well as the amount (in grams) of them that were accepted to compose the dietary regimens. In brief, we started by providing 2.0 g of all substrates, which were only partially taken to the garden; then, we gradually adjusted this amount to reach a quantity that was completely added to the garden. We empirically verified that in colonies having gardens of ~1000 cm^3, workers

Table 2 | Score scale

Aspect	Score	Description
Acceptance		Approximate proportion of substrate cut and added to the garden within 24 h
	5	90–100%
	4	50–80%
	3	30–50%
	2	10–30%
	1	<10%
	0	Dead colony
Garden health		Garden volume (proportion of the 1000 cm^3 chamber occupied when compared to the volume occupied before the experiment), humidity, contamination
	5	Up to 80–100% volume, normal humidity
	4	About 50–80% of volume, normal humidity
	3	About 50% of volume, garden less humid
	2	About 20–50% of volume, garden dark and dry
	1	Volume <20%, garden dark, dry, and contaminated
	0	Dead colony
Decay continuum		Distinctiveness between garden regions (and their volume)
	5	Very well-defined regions with similar thickness
	4	Well defined regions, with the old region being a little thicker
	3	Defined regions, with a thicker old region
	2	Poorly defined regions, with a thicker old region
	1	No defined regions or only old garden
	0	Dead colony
Waste		Waste volume (proportion of chamber occupied), humidity, and microbial overgrowth (observed by naked eye)
	5	<10% of volume, dry, not overgrown by microbes
	4	Up to 10–30% of volume, dry, not overgrown by microbes
	3	About 30–50% of volume, humid, with observable microbial growth
	2	Up to 50–80% of volume, very humid, not overgrown by microbes
	1	Volume >80%, very humid, overgrown by microbes
	0	Dead colony

daily cut and carried to the garden about 0.6 g of leaves, 1.0 g of fruits, or 1.0 g of cereals. These amounts were used as standard for the diet formulation. While fresh leaves were harvested at UNESP Campus, dry leaves, fruits, and cereals were obtained at local stores. All substrates were heat-sterilized by autoclaving (15 min at 121 °C and 1 kgf/cm^2), to minimize the effects of manipulation and substrate-derived microbiota. Fruits were partially dehydrated in a food dehydrator before sterilizing, to avoid their high moisture unbalancing the garden humidity.

Dietary regimens, scoring, and sampling

We took in account substrate diversity for diet formulation, feeding colonies with different substrates each day, since leaf-cutting ants tend to become uninterested in resources provided very repeatedly; besides, we aimed to mimic foraging diversity available in field conditions[215–219]. Dietary treatments included only the accepted substrates during acclimation; thus, all substrates but dry leaves of *E. cinerea* and dry flowers of *H. rosa-sinensis* (not well accepted) were added in the dietary treatments. Colonies ($n = 28$) containing a garden volume of ~1000 cm^3 were randomly assigned to four test groups (containing seven colonies per group), each one receiving, without choice, a standard amount of plant substrates (Supplementary Material) varying in nutritional content and recalcitrance. The four test groups consisted of: 1) Leaves diet: Composed of more recalcitrant substrates, in which ants received about 0.6 g of dry and fresh leaves along 56 days (this was considered the control group, reflecting the leaf-cutting ants' foraging habits in the field). 2) Fruits and cereals diet: Composed of less recalcitrant resources, in which ants were provided with about 1.0 g a selection of dry fruits, oats and rice along 56 days. 3) Generalist diet: Composed of substrates of mixed recalcitrance. Ants were offered, intermittently, leaves (0.6 g) and fruits/cereals (1.0 g) along 56 days. 4) Alternative diet: Ants received leaves (0.6 g) for 20 days, then switched to receive fruits and cereals (1.0 g) until 40 days of experiment, then switched back to leaves (0.6 g) for the last 16 days of experiment. When referring specifically to the gardens of these colonies, we use the terms Leaves, Fruits/cereals, Generalist, and Alternative gardens. Colonies functioning was inferred qualitatively by rating, according to a standard score scale (Table 2, modified from Barcoto et al.[220]), the substrate acceptance, garden health conditions, substrate decay continuum, and waste volume. Colonies were fed daily, at around 9 am, when they were scored. On each day, the four test groups were statistically compared by Friedman's two-way ANOVA by ranks, with a post-hoc test for Friedman[220] using R version 4.4.1 in R Studio [www.R-project.org], for which the command history may be found at the Supplementary Material. Before the experiment (t_0), after 20 days (t_{20}), after 40 days (t_{40}), and after 56 days (t_{56}) of experiment, we sampled ~2.0 g of garden (comprising a composite sample of young, central, and old garden regions) and waste at each time point. Workers and offspring were manually removed using entomological forceps, and garden regions were set apart. Young, central, and old gardens, as well as waste samples were taken for ^{13}C Solid-state Nuclear Magnetic Resonance (^{13}C ssNMR), metabarcoding, and SEM analysis.

Chemical profiles of fungus gardens

The sensitivity of ^{13}C ssNMR to modifications in chemical composition and changes in local microstructures[221–223] makes it suited for elucidating the garden and waste chemical profiles. Samples were pooled by: region (young, central, old, waste), diet (leaves, fruits/cereals, generalist, alternative), and time point (t_0, t_{20}, t_{40}, t_{56}). Pooling resulted in 64 samples (4 regions × 4 diets × 4 time points), which were freeze-dried. Dried samples were analyzed using a Bruker Avance 400 MHz NMR spectrometer, equipped with a Bruker 4-mm magic angle spinning (MAS) double-resonance probehead, at ^{13}C and ^{1}H frequencies of 100.5 MHz and 400.0 MHz, respectively. Spectra of components were extracted using The Unscrambler X ® v10.4.1 (CAMO Software AS). Typical polysaccharide and lignin peaks were assigned following the literature[221].

High-resolution ^{13}C solid state NMR spectra were acquired using ^{1}H–^{13}C Cross-polarization excitation under MAS and high-power ^{1}H decoupling (^{13}C-CPMAS). The typical experimental parameters were a cross-polarization time of 1 ms, a recycle delay of 2 s, ^{1}H and ^{13}C pulse lengths of 3.3 µs and 4.0 µs, respectively, and ^{1}H decoupling amplitude of $gB_1/2\pi = 70$ kHz (SPINAL pulse scheme). Due to its sensitivity to local mobility and abundance of ^{1}H around the ^{13}C nuclei, the ^{13}C-CPMAS method is not quantitative in terms of the absolute number of chemical components. However, if the samples have a similar overall composition and identical acquisition parameters are used, spectra normalized by total spectral intensity (spectral area) can reveal changes in the relative amounts of each type of component by directly comparing intensities within the same spectral regions, i.e., changes in the intensity profile. This applies to the present analysis, where the overall composition of the samples is similar, and the same acquisition parameters were used in all measurements.

^{13}C CPMAS spectra are not strictly quantitative, since the intensity depends on the local ^{1}H density around the ^{13}C nuclei. Yet, comparisons between signals corresponding to the same type of carbon in similar molecular environments (i.e., similar ^{1}H density) are still meaningful. Under these conditions, the relative areas of the two lines reflect the relative amount

of each type of carbon in the sample. Accordingly, by comparing the areas of the two aforementioned lines, one can estimate the relative proportion of C1 carbons in hemicellulose to those in cellulose. The ratio of these two lines provided an estimate of the hemicellulose:cellulose ratio in the samples. In some cases, however, the two-component deconvolution could not be reliably performed due to the presence of sharp additional peaks in the same spectral region. These peaks were likely associated with small-molecule metabolites present in the samples, but their precise assignment could not be made. In such cases, the deconvolution was carried out using three lines, with the area of the unknown sharp peak disregarded, and the hemicellulose:cellulose ratio calculated only from the remaining lines.

DNA extraction, sequencing, and bioinformatic analyses

We randomly selected three out of the seven colonies per diet to analyze the microbial taxonomic composition. Separated by diet and time points, the total DNA of 192 samples (3 colonies × 4 regions × 4 diets × 4 time points) was extracted using the PowerLyzer PowerSoil DNA isolation kit (Qiagen). DNA concentration was quantified by a NanoDrop Lite Spectrophotometer (Thermo Fisher Scientific). Sequencing was carried out on an Illumina HiSeq 2500 platform, generating 2 × 100 bp (200 cycles) paired-end reads, with at least 100,000 sequences per sample at Novogene Corporation Inc. For the bacterial community, the region v3-v4 of 16S rRNA was amplified using the primers 341F (CCTAYGGGRBGCASCAG) and 806R (GGACTACNNGGGTATCTAAT), generating amplicons of ~450–550 base pairs. The fungal community was accessed by amplifying the ITS2 region, using the primers ITS3-2024F (GCATCGATGAAGAACGCAGC) and ITS4-2409R (TCCTCCGCTTATTGATATGC), generating amplicons of ~380 base pairs. To improve sequence quality, ITS amplicons were purified before sequencing using a lysis-binding procedure (performed at Novogene). Briefly, samples were lysed using a lysis buffer, incubated at 55–60 °C for 10–15 min. The supernatant was transferred to a new tube, to which a binding buffer (or ethanol) was added to the lysate. The mixture was applied to a silica column, centrifuged, and then washed by a washing buffer. Elution was carried out by adding an elution buffer, incubated for 1–5 min, and then centrifuged. Even with purification, not all samples were successfully sequenced, which is the reason why the fungal community analysis was not carried out in separated time points. 16S rRNA and ITS rRNA sequences were archived at NCBI, and available under the BioProject ID PRJNA1245348.

Sequences were preprocessed using QUIIME 2 (v2024.5.0)[224]. Demultiplexing and quality control checking were performed by DADA2[225], employing consensus methods for filtering out chimeric sequences and low-quality ones (<q20). 16S rRNA sequencing yielded ~33,389,000 reads, with an average of 173,900 per sample. Sequences were later rarefied to 90,700 based on the lowest number of sequences per sample, with singletons and doubletons being removed. Taxonomic classification of the 16S rRNA regions was carried out using the SILVA Database (version 138), with 97% of similarity[226]. ASVs assigned as "mitochondria" and "chloroplast" were not considered for the following analysis. ITS rRNA sequencing yielded ~18,791,500 reads, with an average of 157,900 per sample. Sequences were rarefied to 38,700 based on the lowest number of sequences per sample, with singletons and doubletons being removed. Taxonomic classification of ITS rRNA was carried out using the UNITE Database, with 97% of similarity[227]. Both 16S and ITS rRNA ASVs were analyzed in MicrobiomeAnalyst[228–230], both by the webserver and by the R package MicrobiomeAnalystR. Features with low count (minimum count = 4, prevalence in samples = 10%) and low variance (10%, based on inter-quantile range) were filtered out, and data was normalized to total sum scaling (TSS normalization). For 16S rRNA ASVs, the relative abundance was profiled at phylum and genus levels; for ITS rRNA ASVs, the relative abundance was determined at the levels of phylum, family, and genus. Differences between the microbiota taxonomic composition were determined by comparing pairs of diets (i. e., two groups) at a time, using the heat tree analysis at genus level, employing the Metacoder package[231] (implemented in the MicrobiomeAnalyst workflow). Heat tree analysis was performed for pairwise comparisons between diets, using the non-parametric Wilcoxon Rank Sum test (p-value cutoff = 0.05) followed by a Benjamini–Hochberg (FDR) correction. Based on the heat trees results, we categorized bacterial and fungal genera as: metabolically adaptable, leaf-favored, fruit-favored, and favored by mixed fibers. A given microbe was considered "favored" by one (or more) diets when it was differentially abundant in that diet, in all pairwise comparisons. Alpha-Diversity was calculated at genus level, for the following diversity metrics: Observed Features (Richness), Shannon, Simpson, and Fisher, testing for significant differences between groups for each diversity index using Mann–Whitney/Kruskal–Wallis, and Wilcoxon test for post hoc pairwise comparisons. Beta-Diversity was calculated at the genus level, with Principal Coordinates Analysis (PCoA) as ordination method, based on Bray–Curtis distances; statistical significance of data distribution and pairwise comparisons were defined by Permuted multivariate ANOVA (PERMANOVA). P-values were corrected by the Benjamini–Hochberg method, with false discovery rate (FDR) ≤ 0.05 being considered statistically significant. The command history of these analyses is available at the Supplementary Material. To estimate the contributions of each microbial taxa to the overall dissimilarity between diets, pairwise analysis of similarity percentage (SIMPER) based on the Bray-Curtis dissimilarities was performed in PAST Version 4.17[232].

Spatial distribution of microbiota across garden regions

Samples were pooled as described for ^{13}C NMR analysis; preparation and image acquisition of the 64 samples were carried out as described in Barcoto et al.[65]. Briefly, samples were fixed for at minimum 24 h in Karnovsky solution (2.5% glutaraldehyde and 2% paraformaldehyde in 0.05 M cacodylate buffer, pH 7.2), maintained at 4 °C. Fixed samples were dehydrated by ethanol gradual washing series (30%, 50%, 70%, 90%, and three times in 100%) and critical point-dried (EM CPD 300). Fragments of dried samples, no larger than 1 mm^3 in size, were mounted in aluminum stubs, adding up to nine fragments per stub, which were sputter-coated with colloidal gold (Baltec SCD 050). Images were visualized and digitally registered using a JEOL IT300 SEM. We recorded about 15–25 images per sample, ranging the following magnifications: i) 100×–700× to observe hyphal density, substrate visual deterioration, and colonization patterns); ii) 700×–1500× to detail microbial spatial organization; iii) 1500×–3000× to describe physical interactions (in special, biofilm structure); iv) 3000×–4000× to focus on informative microbial assemblages. Resulting images were visually analyzed to characterize garden features, and which of these faced changes along the experiment. Such features included: hyphal density, presence of gongylidia, signs of substrate deterioration, substrate-colonizing microbiota (including spread and 3D biofilms), hyphae-colonizing microbiota, and presence of yeasts (Fig. 4A). Each feature was categorized, according to its approximate frequency, as: 0 - extremely rare or not observed; 1 - observed in low abundance; 2 - observed in moderate abundance; 3 - observed in abundance; 4 - observed in high abundance[31].

Data availability

The datasets supporting the conclusions of this article are available in the FigShare repository, under the Project "You are what your fungus eats". NMR spectra may be accessed by https://doi.org/10.6084/m9.figshare.28669955, SEM images by https://doi.org/10.6084/m9.figshare.28670123, score tables and diet details by https://doi.org/10.6084/m9.figshare.28669865. ASV sequences are available at the NCBI repository, under the BioProject ID PRJNA1245348.

Received: 24 April 2025; Accepted: 20 November 2025;
Published online: 18 December 2025

References

1. Elton, C. *Animal Ecology* (Sidwick & Jackson, 1927).
2. Behmer, S. T. Insect herbivore nutrient regulation. *Annu. Rev. Entomol.* **54**, 165–187 (2009).
3. Raubenheimer, D. et al. An integrative approach to dietary balance across the life course. *iScience* **25**, 104315 (2022).

4. Trevelline, B. K. & Kohl, K. D. The gut microbiome influences host diet selection behavior. *Proc. Natl. Acad. Sci. USA* **119**, e2117537119 (2022).
5. Simpson, S. J. & Raubenheimer, D. The nature of nutrition: a unifying framework. *Aust. J. Zool.* **59**, 350–368 (2012).
6. Simpson, S. J. & Raubenheimer, D. Nutritional ecology and human health. *Annu. Rev. Nutr.* **36**, 603–626 (2016).
7. Alcock, J., Maley, C. C. & Aktipis, C. A. Is eating behavior manipulated by the gastrointestinal microbiota? Evolutionary pressures and potential mechanisms. *Bioessays* **36**, 940–949 (2014).
8. McFall-Ngai, M. et al. Animals in a bacterial world, a new imperative for the life sciences. *Proc. Natl. Acad. Sci. USA* **110**, 3229–3236 (2013).
9. Mattson, W. J. Herbivory in relation to plant nitrogen content. *Annu. Rev. Ecol. Evol. Syst.* **11**, 119–161 (1980).
10. Kohl, K. D. et al. Gut microbes of mammalian herbivores facilitate intake of plant toxins. *Ecol. Lett.* **17**, 1238–1246 (2014).
11. Gilbert, S. F. Developmental symbiosis facilitates the multiple origins of herbivory. *Evol. Dev.* **22**, 154–164 (2020).
12. Bigger, D. S. & Marvier, M. A. How different would a world without herbivory be? A search for generality in ecology. *Integr. Biol.* **1**, 60–67 (1998).
13. Maron, J. L. & Crone, E. Herbivory: effects on plant abundance, distribution and population growth. *Proc. R. Soc. B* **273**, 2575–2584 (2006).
14. Cragg, S. M. et al. Lignocellulose degradation mechanisms across the Tree of Life. *Curr. Opin. Chem. Biol.* **29**, 108–119 (2015).
15. Pauly, M. & Keegstra, K. Physiology and metabolism 'Tear down this wall. *Curr. Opin. Plant Biol.* **11**, 233–235 (2008).
16. Bredon, M. et al. Lignocellulose degradation at the holobiont level: teamwork in a keystone soil invertebrate. *Microbiome* **6**, 1–19 (2018).
17. Lillington, S. P. et al. Nature's recyclers: anaerobic microbial communities drive crude biomass deconstruction. *Curr. Opin. Biotechnol.* **62**, 38–47 (2020).
18. Peng, Q. et al. Unraveling the roles of coastal bacterial consortia in degradation of various lignocellulosic substrates. *mSystems* **8**, e01283-22 (2023).
19. Kane, M. D. Microbial fermentation in insect guts. In Gastrointestinal Microbiology: Gastrointestinal Ecosystems and Fermentations (eds, Mackie, R. I., White, B. A. & Isaacson, R. E.) 231–265 (Springer, 1997).
20. Dearing, M. D. & Kohl, K. D. Beyond fermentation: other important services provided to endothermic herbivores by their gut microbiota. *Integr. Comp. Biol.* **57**, 723–731 (2017).
21. Moraïs, S. & Mizrahi, I. The road not taken: the rumen microbiome, functional groups, and community states. *Trends Microbiol.* **27**, 538–549 (2019).
22. Xiao, K. et al. Adaptation of gut microbiome and host metabolic systems to lignocellulosic degradation in bamboo rats. *ISME J.* **16**, 1980–1992 (2022).
23. Liu, H. et al. Ecological dynamics of the gut microbiome in response to dietary fiber. *ISME J.* **16**, 2040–2055 (2022).
24. Mueller, U. G. et al. The evolution of agriculture in insects. *Annu. Rev. Ecol. Evol. Syst.* **36**, 563–595 (2005).
25. Biedermann, P. H. & Veja, F. E. Ecology and evolution of insect–fungus mutualisms. *Annu. Rev. Entomol.* **65**, 431–455 (2020).
26. Li, H. et al. Symbiont-mediated digestion of plant biomass in fungus-farming insects. *Annu. Rev. Entomol.* **66**, 297–316 (2021).
27. Wilson, E. O. The defining traits of fire ants and leaf-cutting ants. In *Fire Ants and Leaf-cutting Ants*, 1–9 (Westview, 1986).
28. Weber, N. A. *Gardening Ants: The Attines* (American Philosophical Society, 1972).
29. Hölldobler, B. & Wilson, E. O. *The Ants* (Harvard University Press, 1990).
30. Folgarait, P. J. Ant biodiversity and its relationship to ecosystem functioning: a review. *Biodivers. Conserv.* **7**, 1221–1244 (1998).
31. Moreira, A. et al. Nest architecture of Atta laevigata (F. Smith, 1858) (Hymenoptera: Formicidae). *Stud. Neotrop. Fauna Environ.* **39**, 109–116 (2004).
32. Herz, H., Beyschlag, W. & Hölldobler, B. Herbivory rate of leaf-cutting ants in a tropical moist forest in Panama at the population and ecosystem scales. *Biotropica* **39**, 482–488 (2007).
33. Leal, I. R., Wirth, R. & Tabarelli, M. The multiple impacts of leaf-cutting ants and their novel ecological role in human-modified neotropical forests. *Biotropica* **46**, 516–528 (2014).
34. Swanson, A. C. et al. Welcome to the *Atta* world: A framework for understanding the effects of leaf-cutter ants on ecosystem functions. *Funct. Ecol.* **33**, 1386–1399 (2019).
35. Hölldobler, B. & Wilson, E. O. *The Leafcutter Ants: Civilization by Instinct* (W.W. Norton and Company Inc., 2011).
36. Römer, D. & Roces, F. Nest enlargement in leaf-cutting ants: relocated brood and fungus trigger the excavation of new chambers. *PLoS One* **9**, e97872 (2014).
37. Farji-Brener, A. G. & Werenkraut, V. A meta-analysis of leaf-cutting ant nest effects on soil fertility and plant performance. *Ecol. Entomol.* **40**, 150–158 (2015).
38. Wirth, R. et al. Herbivory of leaf cutting ants. A case study on *Atta colombica* in the Tropical Rainforest of Panama. In *Ecological Studies Series* (Springer-Verlag, 2003).
39. Mundim, F. M., Costa, A. N. & Vasconcelos, H. L. Leaf nutrient content and host plant selection by leaf-cutter ants, *Atta laevigata*, in a Neotropical savanna. *Entomol. Exp. Appl.* **130**, 47–54 (2009).
40. De Fine Licht, H. H. & Boomsma, J. J. Forage collection, substrate preparation, and diet composition in fungus-growing ants. *Ecol. Entomol.* **35**, 259–269 (2010).
41. Falcão, P. F. et al. Edge-induced narrowing of dietary diversity in leaf-cutting ants. *Bull. Entomol. Res.* **101**, 305–311 (2011).
42. Chapela, I. H. et al. Evolutionary history of the symbiosis between fungus-growing ants and their fungi. *Science* **266**, 1691–1694 (1994).
43. Schultz, T. R. & Brady, S. G. Major evolutionary transitions in ant agriculture. *Proc. Natl. Acad. Sci. USA* **105**, 5435–5440 (2008).
44. De Fine Licht, H. H., Boomsma, J. J. & Tunlid, A. Symbiotic adaptations in the fungal cultivar of leaf-cutting ants. *Nat. Commun.* **5**, 1–10 (2014).
45. Shik, J. Z. et al. Disentangling nutritional pathways linking leafcutter ants and their co-evolved fungal symbionts using stable isotopes. *Ecology* **99**, 1999–2009 (2018).
46. Nygaard, S. et al. Reciprocal genomic evolution in the ant–fungus agricultural symbiosis. *Nat. Commun.* **7**, 12233 (2016).
47. Erthal, M. Jr. et al. Hydrolytic enzymes of leaf-cutting ant fungi. *Comp. Biochem. Physiol. B Biochem. Mol. Biol.* **152**, 54–59 (2009).
48. Aylward, F. O. et al. *Leucoagaricus gongylophorus* produces diverse enzymes for the degradation of recalcitrant plant polymers in leaf-cutter ant fungus gardens. *Appl. Environ. Microbiol.* **79**, 3770–3778 (2013).
49. Moreira-Soto, R. D. et al. Ultrastructural and microbial analyses of cellulose degradation in leaf-cutter ant colonies. *Microbiology* **163**, 1578–1589 (2017).
50. Branstetter, M. G. et al. Dry habitats were crucibles of domestication in the evolution of agriculture in ants. *Proc. Roy. Soc. Lond. Ser. B Biol. Sci.* **284**, 20170095 (2017).
51. Veličković, M. et al. Mapping microhabitats of lignocellulose decomposition by a microbial consortium. *Nat. Chem. Biol.* **20**, 1033–1043 (2024).
52. Leal-Dutra, C. A. et al. Evidence that the domesticated fungus *Leucoagaricus gongylophorus* recycles its cytoplasmic contents as nutritional rewards to feed its leafcutter ant farmers. *IMA Fungus* **14**, 19 (2023).

53. Littledyke, M. & Cherrett, J. M. Direct ingestion of plant sap from cut leaves by leaf-cutting ants *Atta cephalotes* (L.) and *Acromyrmex octospinosus* (Reich) (Formicidae, Attini). *Bull. Entomol. Res.* **66**, 205–217 (1976).
54. Quinlan, R. J. & Cherrett, J. M. The role of fungus in the diet of the leaf-cutting ant Atta cephalotes (L. Ecol. Entomol. 4, 151–160 (1979) .
55. De Fine Licht, H. H. et al. Evolutionary transitions in enzyme activity of ant fungus gardens. *Evolution* **64**, 2055–2069 (2010).
56. Aylward, F. O. et al. Enrichment and broad representation of plant biomass-degrading enzymes in the specialized hyphal swellings of *Leucoagaricus gongylophorus*, the fungal symbiont of leaf-cutter ants. *PloS One* **10**, e0134752 (2015).
57. Khadempour, L. et al. From plants to ants: fungal modification of leaf lipids for nutrition and communication in the leaf-cutter ant fungal garden ecosystem. *mSystems* **6**, 10–1128 (2021).
58. Conlon, B. H. et al. A fungal symbiont converts provisioned cellulose into edible yield for its leafcutter ant farmers. *Biol. Lett.* **18**, 20220022 (2022).
59. Pinto-Tomás, A. A. et al. Symbiotic nitrogen fixation in the fungus gardens of leaf-cutter ants. *Science* **326**, 1120–1123 (2009).
60. Scott, J. J. et al. Microbial community structure of leaf-cutter ant fungus gardens and refuse dumps. *PloS One* **5**, e9922 (2010).
61. Suen, G. et al. An insect herbivore microbiome with high plant biomass-degrading capacity. *PLoS Genet.* **6**, e1001129 (2010).
62. Aylward, F. O. et al. Metagenomic and metaproteomic insights into bacterial communities in leaf-cutter ant fungus gardens. *ISME J.* **6**, 1688–1701 (2012).
63. Aylward, F. O. et al. Convergent bacterial microbiotas in the fungal agricultural systems of insects. *mBio* **5**, 10–1128 (2014).
64. Barcoto, M. O. et al. Fungus-growing insects host a distinctive microbiota apparently adapted to the fungiculture environment. *Sci. Rep.* **10**, 12384 (2020).
65. Barcoto, M. O. et al. Microbiota of attine ants' gardens: Visualizing a microbial landscape by Scanning Electron Microscopy. *J. Vis. Exp.* **212**, e67334 (2024).
66. Francoeur, C. B. et al. Bacteria contribute to plant secondary compound degradation in a generalist herbivore system. *mBio* **11**, 10–1128 (2020).
67. Khadempour, L. et al. Metagenomics reveals diet-specific specialization of bacterial communities in fungus gardens of grass- and dicot-cutter ants. *Front. Microbiol.* **11**, 570770 (2020).
68. Martiarena, M. J. S. et al. The hyphosphere of leaf-cutting ant cultivars is enriched with helper bacteria. *Microb. Ecol.* **86**, 1773–1788 (2023).
69. Donaldson, G. P., Lee, S. M. & Mazmanian, S. K. Gut biogeography of the bacterial microbiota. *Nat. Rev. Microbiol.* **14**, 20–32 (2016).
70. Zeng, Y. et al. Microbial biogeography along the gastrointestinal tract of a red panda. *Front. Microbiol.* **9**, 1411 (2018).
71. Kuramae, E. E. et al. Wood decay characteristics and interspecific interactions control bacterial community succession in *Populus grandidentata* (Bigtooth Aspen). *Front. Microbiol.* **10**, 979 (2019).
72. Hu, X. et al. Gastrointestinal biogeography of luminal microbiota and short-chain fatty acids in sika deer (*Cervus nippon*). *Appl. Environ. Microbiol.* **88**, e00499-22 (2022).
73. Eisenhofer, R. et al. Microbial biogeography of the wombat gastrointestinal tract. *PeerJ* **10**, e12982 (2022).
74. Soltis, M. P. et al. Rumen biogeographical regions and their impact on microbial and metabolome variation. *Front. Anim. Sci.* **4**, 1154463 (2023).
75. Meier, K. H. et al. Metabolic landscape of the male mouse gut identifies different niches determined by microbial activities. *Nat. Metab.* **5**, 968–980 (2023).
76. Adade, E. E. et al. Recent progress in analyzing the spatial structure of the human microbiome: Distinguishing biogeography and architecture in the oral and gut communities. *Curr. Opin. Endocr. Metab. Res.* **18**, 275–283 (2021).
77. Martin, M. M., Carman, R. M. & MacConnell, J. G. Nutrients derived from the fungus cultured by the fungus-growing ant *Atta colombica* tonsipes. *Ann. Entomol. Soc. Am.* **62**, 11–13 (1969).
78. Schiøtt, M. et al. Towards a molecular understanding of symbiont function: identification of a fungal gene for the degradation of xylan in the fungus gardens of leaf-cutting ants. *BMC Microbiol.* **8**, 1–10 (2008).
79. Moller, I. E. et al. The dynamics of plant cell-wall polysaccharide decomposition in leaf-cutting ant fungus gardens. *PLoS One* **6**, e17506 (2011).
80. Grell, M. N. et al. The fungal symbiont of *Acromyrmex* leaf-cutting ants expresses the full spectrum of genes to degrade cellulose and other plant cell wall polysaccharides. *BMC Genom.* **14**, 1–11 (2013).
81. Lange, L. & Grell, M. N. The prominent role of fungi and fungal enzymes in the ant–fungus biomass conversion symbiosis. *Appl. Microbiol. Biotechnol.* **98**, 4839–4851 (2014).
82. North, R. D., Jackson, C. W. & Howse, P. E. Communication between the fungus garden and workers of the leaf-cutting ant, *Atta sexdens rubropilosa*, regarding choice of substrate for the fungus. *Physiol. Entomol.* **24**, 127–133 (1999).
83. Bot, A. N. et al. Waste management in leaf-cutting ants. *Ethol. Ecol. Evol.* **13**, 225–237 (2001).
84. Schiøtt, M. et al. Leaf-cutting ant fungi produce cell wall degrading pectinase complexes reminiscent of phytopathogenic fungi. *BMC Biol.* **8**, 1–12 (2010).
85. Lewin, G. R. et al. Cellulose-enriched microbial communities from leaf-cutter ant (*Atta colombica*) refuse dumps vary in taxonomic composition and degradation ability. *PLoS One* **11**, e0151840 (2016).
86. Kooij, P. W. et al. Rapid shifts in *Atta cephalotes* fungus-garden enzyme activity after a change in fungal substrate (Attini, Formicidae). *Insectes Soc.* **58**, 145–151 (2011).
87. Khadempour, L. et al. The fungal cultivar of leaf-cutter ants produces specific enzymes in response to different plant substrates. *Mol. Ecol.* **25**, 5795–5805 (2016).
88. Jiang, F. et al. Marked seasonal variation in structure and function of gut microbiota in forest and alpine musk deer. *Front. Microbiol.* **12**, 699797 (2021).
89. Wu, Q. et al. Seasonal variation in nutrient utilization shapes gut microbiome structure and function in wild giant pandas. *Proc. R. Soc. B.* **284**, 20170955 (2017).
90. Huang, G. et al. Seasonal shift of the gut microbiome synchronizes host peripheral circadian rhythm for physiological adaptation to a low-fat diet in the giant panda. *Cell Rep.* **38**, 110203 (2022).
91. Baniel, A. et al. Seasonal shifts in the gut microbiome indicate plastic responses to diet in wild geladas. *Microbiome* **9**, 1–20 (2021).
92. Li, Q. et al. Gut microbiome responds compositionally and functionally to the seasonal diet variations in wild gibbons. *NPJ Biofilms Microbi.* **9**, 21 (2023).
93. Hicks, A. L. et al. Gut microbiomes of wild great apes fluctuate seasonally in response to diet. *Nat. Commun.* **9**, 1786 (2018).
94. Li, B. W., Andrews, K. W. & Pehrsson, P. R. Individual sugars, soluble, and insoluble dietary fiber contents of 70 high consumption foods. *J. Food Compos. Anal.* **15**, 715–723 (2002).
95. Brazilian Food Composition Table (TBCA). University of São Paulo (USP). Food Research Center (FoRC). Version 7.2. São Paulo, http://www.fcf.usp.br/tbca (2022).
96. Hamaker, B. R. & Tuncil, Y. E. A perspective on the complexity of dietary fiber structures and their potential effect on the gut microbiota. *J. Mol. Biol.* **426**, 3838–3850 (2014).
97. Gharechahi, J. et al. Functional and phylogenetic analyses of camel rumen microbiota associated with different lignocellulosic substrates. *NPJ Biofilms Microbi.* **8**, 46 (2022).

98. Tom, L. M. et al. Low-abundance populations distinguish microbiome performance in plant cell wall deconstruction. *Microbiome* **10**, 183 (2022).
99. Peng, Q. et al. Unraveling the roles of coastal bacterial consortia in degradation of various lignocellulosic substrates. *mSystems* **8**, e0128322 (2023).
100. Holland, C. et al. Plant cell walls: Impact on nutrient bioaccessibility and digestibility. *Foods* **9**, 201 (2020).
101. Puhlmann, M. L. & de Vos, W. M. Intrinsic dietary fibers and the gut microbiome: Rediscovering the benefits of the plant cell matrix for human health. *Front. Immunol.* **13**, 954845 (2022).
102. Deehan, E. C. et al. Modulation of the gastrointestinal microbiome with nondigestible fermentable carbohydrates to improve human health. *Microbiol. Spectr.* **5**, 10–1128 (2017).
103. Makki, K. et al. The impact of dietary fiber on gut microbiota in host health and disease. *Cell Host Microbe* **23**, 705–715 (2018).
104. Castillo, J. J. et al. The development of the Davis Food Glycopedia - a glycan encyclopedia of food. *Nutrients* **14**, 1639 (2022).
105. De Fine Licht, H. H. et al. Laccase detoxification mediates the nutritional alliance between leaf-cutting ants and fungus-garden symbionts. *Proc. Natl. Acad. Sci. USA* **110**, 583–587 (2013).
106. Kooij, P. W. et al. *Leucoagaricus gongylophorus* uses leaf-cutting ants to vector proteolytic enzymes towards new plant substrate. *ISME J.* **8**, 1032–1040 (2014).
107. Kooij, P. W. et al. Ant mediated redistribution of a xyloglucanase enzyme in fungus gardens of *Acromyrmex echinatior*. *BMC Microbiol.* **16**, 1–9 (2016).
108. Somera, A. et al. Leaf-cutter ant fungus gardens are biphasic mixed microbial bioreactors that convert plant biomass to polyols with biotechnological applications. *Appl. Environ. Microbiol.* **81**, 4525–4535 (2015).
109. Earle, K. A. et al. Quantitative imaging of gut microbiota spatial organization. *Cell Host Microbe* **18**, 478–488 (2015).
110. Riva, A. et al. A fiber-deprived diet disturbs the fine-scale spatial architecture of the murine colon microbiome. *Nat. Commun.* **10**, 4366 (2019).
111. Koropatkin, N. M., Cameron, E. A. & Martens, E. C. How glycan metabolism shapes the human gut microbiota. *Nat. Rev. Microbiol.* **10**, 323–335 (2012).
112. Culp, E. J. & Goodman, A. L. Cross-feeding in the gut microbiome: ecology and mechanisms. *Cell Host Microbe* **31**, 485–499 (2023).
113. Quinn, R. A. et al. Niche partitioning of a pathogenic microbiome driven by chemical gradients. *Sci. Adv.* **4**, eaau1908 (2018).
114. Fierer, N. et al. Guidelines for preventing and reporting contamination in low-biomass microbiome studies. *Nat. Microbiol.* **10**, 1570–1580 (2025).
115. Williamson, E. M., Hammer, T. J., Hogendoorn, K. & Eisenhofer, R. Blanking on blanks: few insect microbiota studies control for contaminants. *mBio* **16**, e02658–24 (2025).
116. Akhtar, N. et al. Characterization of cellulase producing *Bacillus* sp. for effective degradation of leaf litter biomass. *Environ. Prog. Sustain. Energy* **32**, 1195–1201 (2013).
117. Fusco, V. et al. The genus *Weissella*: taxonomy, ecology and biotechnological potential. *Front. Microbiol.* **6**, 155 (2015).
118. Haque, M. A. et al. Rapid deconstruction of cotton, coir, areca, and banana fibers recalcitrant structure using a bacterialconsortium with enhanced saccharification. *Waste Biomass Valori*. **12**, 4001–4018 (2021).
119. Fanelli, F. et al. Novel insights into the phylogeny and biotechnological potential of *Weissella* species. *Front. Microbiol.* **13**, 914036 (2022).
120. Li, Z., Zheng, M., Zheng, J. & Gänzle, M. G. *Bacillus* species in food fermentations: an underappreciated group of organisms for safe use in food fermentations. *Curr. Opin. Food Sci.* **50**, 101007 (2023).
121. Singh, A. K. et al. Identification and comprehensive genomic characterization of cellulolytic *Bacillus* species reveal unique CAZyme profiles for leaf litter degradation and compost production. *World J. Microbiol. Biotechnol.* **41**, 245 (2025).
122. Nakabachi, A., Inoue, H. & Hirose, Y. High-resolution microbiome analyses of nine psyllid species of the family Triozidae identified previously unrecognized but major bacterial populations, including *Liberibacter* and *Wolbachia* of supergroup O. *Microbes Environ.* **37**, ME22078 (2022).
123. Botero, J., Cnockaert, M., Zhang, Y., Peeters, C. & Vandamme, P. *Carnimonas bestiolae* sp. nov. and *Cernens ardua* gen. nov., sp. nov.: new halotolerant bacteria from the invasive solitary bee *Megachile sculpturalis*. *Syst. Appl. Microbiol.* **48**, 126648 (2025).
124. Basharat, S. et al. Bacterial diversity of stingless bee honey in Yunnan, China: isolation and genome sequencing of a novel acid-resistant *Lactobacillus pentosus* (SYBC-MI) with probiotic and L. tryptophan producing potential via millet fermentation. *Front. Bioeng. Biotechnol.* **11**, 1272308 (2023).
125. Liu, H. et al. Microbial diversity in stingless bee gut is linked to host wing size and influenced by the environment. *J. Invertebr. Pathol.* **198**, 107909 (2023).
126. Anderson, K. E. et al. Microbial ecology of the hive and pollination landscape: bacterial associates from floral nectar, the alimentary tract and stored food of honey bees (*Apis mellifera*). *PloS One* **8**, e83125 (2013).
127. Iorizzo, M. et al. Diversity of plant pollen sources, microbial communities, and phenolic compounds present in bee pollen and bee bread. *Environ. Sci. Pollut. Res.* **32**, 10425–10435 (2024).
128. Tang, Q. H. et al. The composition of bacteria in gut and beebread of stingless bees (Apidae: Meliponini) from tropics Yunnan, China. *Antonie Van. Leeuwenhoek* **114**, 1293–1305 (2021).
129. Zani, R. D. O. A., Ferro, M. & Bacci, M. Jr. Three phylogenetically distinct and culturable diazotrophs are perennial symbionts of leaf-cutting ants. *Evol. Ecol.* **11**, 17686–17699 (2021).
130. Chen, M. et al. Enhanced heterotrophic nitrification and aerobic denitrification performance of *Glutamicibacter arilaitensis* EM-H8 with different carbon sources. *Chemosphere* **323**, 138266 (2023).
131. Kumari, S. & Naraian, R. Enhanced growth and yield of oyster mushroom by growth-promoting bacteria *Glutamicibacter arilaitensis* MRC119. *J. Basic Microbiol.* **61**, 45–54 (2021).
132. Behrendt, U., Ulrich, A. & Schumann, P. *Leucobacter tardus* sp. nov., isolated from the phyllosphere of *Solanum tuberosum* L. *Int. J. Syst. Evol. Microbiol.* **58**, 2574–2578 (2008).
133. Schäfer, M. et al. Mapping phyllosphere microbiota interactions *in planta* to establish genotype–phenotype relationships. *Nat. Microbiol.* **7**, 856–867 (2022).
134. Wolf, A. et al. *Stenotrophomonas rhizophila* sp. nov., a novel plant-associated bacterium with antifungal properties. *Int. J. Syst. Evol. Microbiol.* **52**, 1937–1944 (2002).
135. Lin, P. et al. *Paracoccus hibiscisoli* sp. nov., isolated from the rhizosphere of Mugunghwa (*Hibiscus syriacus*). *Int. J. Syst. Evol. Microbiol.* **67**, 2452–2458 (2017).
136. Ryan, R. P. et al. The versatility and adaptation of bacteria from the genus *Stenotrophomonas*. *Nat. Rev. Microbiol.* **7**, 514–525 (2009).
137. Coelho, B. D. et al. Bioaugmentation with *Advenella kashmirensis* for the treatment of a kraft pulp effluent by aerated lagoon. *Rev. Ambient. Água* **19**, e2935 (2024).
138. Kim, K. K., Park, H. Y., Park, W., Kim, I. S. & Lee, S. T. *Microbacterium xylanilyticum* sp. nov., a xylan-degrading bacterium isolated from a biofilm. *Int. J. Syst. Evol. Microbiol.* **55**, 2075–2079 (2005).
139. Park, H. Y., Kim, K. K., Jin, L. & Lee, S. T. *Microbacterium paludicola* sp. nov., a novel xylanolytic bacterium isolated from swamp forest. *Int. J. Syst. Evol. Microbiol.* **56**, 535–539 (2006).
140. López-Mondéjar, R. et al. Decoding the complete arsenal for cellulose and hemicellulose deconstruction in the highly efficient

cellulose decomposer *Paenibacillus* O199. *Biotechnol. Biofuels* **9**, 104 (2016).
141. Qiu, Y. et al. A strain of *Paenibacillus polysaccharolyticus* XY5 promotes fiber component degradation in a co-fermentation system of mulberry leaves and distillers' grains. *Lett. Appl. Microbiol.* **78**, ovaf058 (2025).
142. Tang, H., Li, Y. Q., Zheng, L., Wang, M. J. & Luo, C. B. Efficient saccharification of bamboo biomass by secretome protein of the cellulolytic bacterium *Serratia marcescens* LY1 based on whole-genome and secretome analysis. *Renew. Energy* **193**, 32–40 (2022).
143. Hsu, C. L. et al. Pretreatment and hydrolysis of cellulosic agricultural wastes with a cellulase-producing *Streptomyces* for bioethanol production. *Biomass Bioenergy* **35**, 1878–1884 (2011).
144. Wibberg, D. et al. Complete genome sequence of *Streptomyces reticuli*, an efficient degrader of crystalline cellulose. *J. Biotech.* **222**, 13–14 (2016).
145. Zhang, Y., Hu, J., Tan, H., Zhong, Y. & Nie, S. *Akkermansia muciniphila*, an important link between dietary fiber and host health. *Curr. Opin. Food Sci.* **47**, 100905 (2022).
146. Warnick, T. A., Methe, B. A. & Leschine, S. B. *Clostridium phytofermentans* sp. nov., a cellulolytic mesophile from forest soil. *Int. J. Syst. Evol. Microbiol.* **52**, 1155–1160 (2002).
147. Koukiekolo, R. et al. Degradation of corn fiber by *Clostridium cellulovorans* cellulases and hemicellulases and contribution of scaffolding protein CbpA. *Appl. Environ. Microbiol* **71**, 3504–3511 (2005).
148. Dürre, P. Physiology and sporulation in *Clostridium*. *Microbiol. Spectr.* **2**, 10–1128 (2014).
149. Ouwerkerk, J. P. et al. Adaptation of *Akkermansia muciniphila* to the oxic-anoxic interface of the mucus layer. *Appl. Environ. Microbiol.* **82**, 6983–6993 (2016).
150. Kreisel, H. Fungi from fungus gardens of *Atta insularis* in Cuba. *Z. Allg. Mikrobiol.* **12**, 643–654 (1972).
151. Bass, M. & Cherrett, J. M. The role of leaf-cutting ant workers (Hymenoptera: Formicidae) in fungus garden maintenance. *Ecol. Entomol.* **19**, 215–220 (1994).
152. Montoya, Q. V. et al. Taxonomy and systematics of the fungus-growing ant associate *Escovopsis* (*Hypocreaceae*). *Stud. Mycol.* **106**, 349–397 (2023).
153. Giraldo, C. et al. Yeasts associated with the worker caste of the leaf-cutting ant *Atta cephalotes* under experimental conditions in Colombia. *Arch. Microbiol.* **204**, 284 (2022).
154. Bizarria, R. et al. Uncovering the yeast communities in fungus-growing ant colonies. *Microb. Ecol.* **86**, 624–635 (2023).
155. Pagnocca, F. C. et al. Yeasts isolated from a fungus-growing ant nest, including the description of *Trichosporon chiarellii* sp. nov., an anamorphic basidiomycetous yeast. *Int. J. Syst. Evol. Microbiol.* **60**, 1454–1459 (2010).
156. Melo, W. G. et al. Yeasts in the nests of the leaf-cutter ant *Acromyrmex balzani* in a Savanna biome: exploitation of community and metabolic diversity. *Antonie Van. Leeuwenhoek* **114**, 751–764 (2021).
157. Lievens, B. et al. Microbiology of sugar-rich environments: diversity, ecology and system constraints. *Environ. Microbiol.* **17**, 278–298 (2015).
158. Aro, N., Pakula, T. & Penttilä, M. Transcriptional regulation of plant cell wall degradation by filamentous fungi. *FEMS Microbiol. Rev.* **29**, 719–739 (2005).
159. Daly, P. et al. Glucose-mediated repression of plant biomass utilization in the white-rot fungus *Dichomitus squalens*. *Appl. Environ. Microbiol.* **85**, e01828-19 (2019).
160. Llanos, A. et al. Carbon sources and XlnR-dependent transcriptional landscape of CAZymes in the industrial fungus *Talaromyces versatilis*: when exception seems to be the rule. *Microb. Cell Fact.* **18**, 1–25 (2019).
161. Saltarelli, R. et al. A high concentration of glucose inhibits *Tuber borchii* mycelium growth: a biochemical investigation. *Mycol. Res.* **107**, 72–76 (2003).
162. Kusuda, M. et al. Effects of carbohydrate substrate on the vegetative mycelial growth of an ectomycorrhizal mushroom, *Tricholoma matsutake*, isolated from *Quercus*. *Mycoscience* **48**, 358–364 (2007).
163. Creti, R. et al. Enterococcal colonization of the gastro-intestinal tract: role of biofilm and environmental oligosaccharides. *BMC Microbiol.* **6**, 1–8 (2006).
164. Negrini, T. D. C. et al. Dietary sugars modulate bacterial-fungal interactions in saliva and inter-kingdom biofilm formation on apatitic surface. *Front. Cell Infect. Microbiol.* **12**, 993640 (2022).
165. Yao, S. et al. Sucrose contributed to the biofilm formation of *Tetragenococcus halophilus* and changed the biofilm structure. *Food Microbiol.* **124**, 104616 (2024).
166. Papp, K., Hungate, B. A. & Schwartz, E. Glucose triggers strong taxon-specific responses in microbial growth and activity: insights from DNA and RNA qSIP. *Ecology* **101**, e02887 (2020).
167. Cárdenas, A. et al. Excess labile carbon promotes the expression of virulence factors in coral reef bacterioplankton. *ISME J.* **12**, 59–76 (2018).
168. Goldford, J. E. et al. Emergent simplicity in microbial community assembly. *Science* **361**, 469–474 (2018).
169. Khan, S. et al. Dietary simple sugars alter microbial ecology in the gut and promote colitis in mice. *Sci. Transl. Med.* **12**, eaay6218 (2020).
170. Pan, Y. et al. Carbon source shaped microbial ecology, metabolism and performance in denitrification systems. *Water Res.* **243**, 120330 (2023).
171. Shik, J. Z. et al. Nutrition mediates the expression of cultivar–farmer conflict in a fungus-growing ant. *Proc. Natl. Acad. Sci. USA* **113**, 10121–10126 (2016).
172. Shik, J. Z. et al. Nutritional niches reveal fundamental domestication trade-offs in fungus-farming ants. *Nat. Ecol. Evol.* **5**, 122–134 (2021).
173. Herz, H., Hölldobler, B. & Roces, F. Delayed rejection in a leaf-cutting ant after foraging on plants unsuitable for the symbiotic fungus. *Behav. Ecol.* **19**, 575–582 (2008).
174. Hubbell, S. P., Wiemer, D. F. & Adejare, A. An antifungal terpenoid defends a neotropical tree (Hymenaea) against attack by fungus-growing ants (*Atta*). *Oecologia* **60**, 321–327 (1983).
175. Hubbell, S. P., Howard, J. J. & Wiemer, D. F. Chemical leaf repellency to an attine ant: seasonal distribution among potential host plant species. *Ecology* **65**, 1067–1076 (1984).
176. Ridley, P., Howse, P. E. & Jackson, C. W. Control of the behavior of leaf-cutting ants by their 'symbiotic' fungus. *Experientia* **52**, 631–635 (1996).
177. Saverschek, N. et al. Avoiding plants unsuitable for the symbiotic fungus: learning and long-term memory in leaf-cutting ants. *Anim. Behav.* **79**, 689–698 (2010).
178. Goes, A. C. et al. How do leaf-cutting ants recognize antagonistic microbes in their fungal crops?. *Front. Ecol. Evol.* **8**, 95 (2020).
179. Kyle, K. E. et al. *Trachymyrmex septentrionalis* ants promote fungus garden hygiene using *Trichoderma*-derived metabolite cues. *Proc. Natl. Acad. Sci. USA* **120**, e2219373120 (2023).
180. Teseo, S. et al. The scent of symbiosis: gut bacteria may affect social interactions in leaf-cutting ants. *Anim. Behav.* **150**, 239–254 (2019).
181. Liberti, J. et al. The gut microbiota affects the social network of honeybees. *Nat. Ecol. Evol.* **6**, 1471–1479 (2022).
182. Scherlach, K. & Hertweck, C. Chemical mediators at the bacterial-fungal interface. *Annu. Rev. Microbiol.* **74**, 267–290 (2020).
183. Lozano, G. L. et al. Introducing THOR, a model microbiome for genetic dissection of community behavior. *mBio* **10**, 10–128 (2020).
184. Kern, L. et al. Commensal inter-bacterial interactions shaping the microbiota. *Curr. Opin. Microbiol.* **63**, 158–171 (2021).
185. Graf, J. Lessons from digestive-tract symbioses between bacteria and invertebrates. *Annu. Rev. Microbiol.* **70**, 375–393 (2016).

186. Chevrette, M. G. et al. Microbiome composition modulates secondary metabolism in a multispecies bacterial community. *Proc. Natl. Acad. Sci. USA* **119**, e2212930119 (2022).
187. Srinivasan, S., Jnana, A. & Murali, T. S. Modeling microbial community networks: methods and tools for studying microbial interactions. *Microb. Ecol.* **87**, 56 (2024).
188. Mark Welch, J. L. et al. Biogeography of a human oral microbiome at the micron scale. *Proc. Natl. Acad. Sci. USA* **113**, E791–E800 (2016).
189. Morales, D. P. et al. Advances and challenges in fluorescence in situ hybridization for visualizing fungal endobacteria. *Front. Microbiol.* **13**, 892227 (2022).
190. Shi, H. et al. Highly multiplexed spatial mapping of microbial communities. *Nature* **588**, 676–681 (2020).
191. Valm, A. M., Welch, J. L. & Borisy, G. G. CLASI-FISH: principles of combinatorial labeling and spectral imaging. *Syst. Appl. Microbiol.* **35**, 496–502 (2012).
192. Fernandez-Brime, S. et al. Bacterial communities in an optional lichen symbiosis are determined by substrate, not algal photobionts. *FEMS Microbiol. Ecol.* **95**, fiz012 (2019).
193. Schlüter, S., Eickhorst, T. & Mueller, C. W. Correlative imaging reveals holistic view of soil microenvironments. *Environ. Sci. Technol.* **53**, 829–837 (2018).
194. Garg, N. et al. Three-dimensional microbiome and metabolome cartography of a diseased human lung. *Cell Host Microbe* **22**, 705–716 (2017).
195. Bouslimani, A. et al. Molecular cartography of the human skin surface in 3D. *Proc. Natl. Acad. Sci. USA* **112**, E2120–E2129 (2015).
196. Brunetti, A. E. et al. An integrative omics perspective for the analysis of chemical signals in ecological interactions. *Chem. Soc. Rev.* **47**, 1574–1591 (2018).
197. Baker, N. R. et al. Nutrient and moisture limitations reveal keystone metabolites linking rhizosphere metabolomes and microbiomes. *Proc. Natl. Acad. Sci. USA* **121**, e2303439121 (2024).
198. Gould, A. L. et al. Microbiome interactions shape host fitness. *Proc. Natl. Acad. Sci. USA* **115**, E11951–E11960 (2018).
199. Brunetti, A. E. et al. Symbiotic skin bacteria as a source for sex-specific scents in frogs. *Proc. Natl. Acad. Sci. USA* **116**, 2124–2129 (2019).
200. Petersen, C. & Round, J. L. Defining dysbiosis and its influence on host immunity and disease. *Cell Microbiol.* **16**, 1024–1033 (2014).
201. Sonnenburg, E. D. & Sonnenburg, J. L. Starving our microbial self: the deleterious consequences of a diet deficient in microbiota-accessible carbohydrates. *Cell Metab.* **20**, 779–786 (2014).
202. Marasco, R. et al. Destabilization of the bacterial interactome identifies nutrient restriction-induced dysbiosis in insect guts. *Microbiol. Spectr.* **10**, e01580-21 (2022).
203. Jin, C. et al. Multi-omics reveal mechanisms of high enteral starch diet mediated colonic dysbiosis via microbiome-host interactions in young ruminant. *Microbiome* **12**, 38 (2024).
204. Hooks, K. B. & O'Malley, M. A. Dysbiosis and its discontents. *mBio* **8**, 10–1128 (2017).
205. Kelley, D. The conceptual ecology of "dysbiosis". *Biol. Theory*. **19**, 221–223 (2024).
206. Olesen, S. W. & Alm, E. J. Dysbiosis is not an answer. *Nat. Microbiol.* **1**, 1–2 (2016).
207. Lachnit, T., Bosch, T. C. & Deines, P. Exposure of the host-associated microbiome to nutrient-rich conditions may lead to dysbiosis and disease development - an evolutionary perspective. *mBio* **10**, 10–1128 (2019).
208. Illiano, P., Brambilla, R. & Parolini, C. The mutual interplay of gut microbiota, diet and human disease. *FEBS J.* **287**, 833–855 (2020).
209. D'Angelo, C. & Wiedenmann, J. Impacts of nutrient enrichment on coral reefs: new perspectives and implications for coastal management and reef survival. *Curr. Opin. Environ. Sustain.* **7**, 82–93 (2014).
210. Zaneveld, J. R. et al. Overfishing and nutrient pollution interact with temperature to disrupt coral reefs down to microbial scales. *Nat. Commun.* **7**, 1–12 (2016).
211. Lachnit, T. et al. Nutrition-induced changes in the microbiota can cause dysbiosis and disease development. *mBio* **16**, e03843-24 (2025).
212. Li, J. M. et al. Dietary fructose-induced gut dysbiosis promotes mouse hippocampal neuroinflammation: a benefit of short-chain fatty acids. *Microbiome* **7**, 1–14 (2019).
213. Winter, S. E. & Bäumler, A. J. Gut dysbiosis: ecological causes and causative effects on human disease. *Proc. Natl. Acad. Sci. USA* **120**, e2316579120 (2023).
214. Saverschek, N. & Roces, F. Foraging leafcutter ants: olfactory memory underlies delayed avoidance of plants unsuitable for the symbiotic fungus. *Anim. Behav.* **82**, 453–458 (2011).
215. Nogueira, B. R. et al. Collection and long-term maintenance of leaf-cutting ants (*Atta*) in laboratory conditions. *J. Vis. Exp*. **186**, e64154 (2022).
216. Wetterer, J. K. Ontogenetic changes in forager polymorphism and foraging ecology in the leaf-cutting ant *Atta cephalotes*. *Oecologia* **98**, 235–238 (1994).
217. Wetterer, J. K. Forager polymorphism, size-matching, and load delivery in the leaf-cutting ant, *Atta cephalotes*. *Ecol. Entomol.* **19**, 57–64 (1994).
218. Franze, C. & Farji-Brener, A. G. Oportunistas o selectivas? Plasticidad en la dieta de la hormiga cortadora de hojas *Acromyrmex lobicornis* en el noroeste de la Patagonia. *Ecol. Austral* **10**, 159–168 (2000).
219. Camargo, R. S. et al. Post-selection and return of foraged material by *Acromyrmex subterraneus brunneus*. *Sociobiology* **42**, 93–102 (2003).
220. Barcoto, M. O. et al. Pathogenic nature of *Syncephalastrum* in *Atta sexdens rubropilosa* fungus gardens. *Pest Manag. Sci.* **73**, 999–1009 (2017).
221. Rezende, C. A. et al. Chemical and morphological characterization of sugarcane bagasse submitted to a delignification process for enhanced enzymatic digestibility. *Biotechnol. Biofuels* **4**, 1–19 (2011).
222. Bernardinelli, O. D. et al. Quantitative 13C MultiCP solid-state NMR as a tool for evaluation of cellulose crystallinity index measured directly inside sugarcane biomass. *Biotechnol. Biofuels* **8**, 110 (2015).
223. Simmons, T. J. et al. Folding of xylan onto cellulose fibrils in plant cell walls revealed by solid-state NMR. *Nat. Commun.* **7**, 13902 (2016).
224. Bolyen, E. et al. Reproducible, interactive, scalable and extensible microbiome data science using QIIME 2. *Nat. Biotechnol.* **37**, 852–857 (2019).
225. Callahan, B. J. et al. DADA2: high-resolution sample inference from Illumina amplicon data. *Nat. Methods* **13**, 581–583 (2016).
226. Quast, C. et al. The SILVA ribosomal RNA gene database project: improved data processing and web-based tools. *Nucleic Acids Res.* **41**, D590–D596 (2012).
227. Abarenkov, K. et al. The UNITE database for molecular identification and taxonomic communication of fungi and other eukaryotes: sequences, taxa and classifications reconsidered. *Nucleic Acids Res.* **52**, D791–D797 (2024).
228. Dhariwal, A. et al. MicrobiomeAnalyst: a web-based tool for comprehensive statistical, visual and meta-analysis of microbiome data. *Nucleic Acids Res.* **45**, W180–W188 (2017).
229. Chong, J. et al. Using MicrobiomeAnalyst for comprehensive statistical, functional, and meta-analysis of microbiome data. *Nat. Protoc.* **15**, 799–821 (2020).
230. Lu, Y. et al. MicrobiomeAnalyst 2.0: comprehensive statistical, functional and integrative analysis of microbiome data. *Nucleic Acids Res.* **51**, W310–W318 (2023).

231. Foster, Z. S., Sharpton, T. J. & Grunwald, N. J. Metacoder: an R package for visualization and manipulation of community taxonomic diversity data. *PLoS Comput. Biol.* **13**, e1005404 (2017).
232. Hammer, Ø. & Harper, D. A. Past: paleontological statistics software package for education and data analysis. *Palaeontol. Electron.* **4**, 1 (2001).

Acknowledgements

The authors would like to thank Elliot Watanabe Kitajima for constructive comments on SEM analysis and to Renato Barbosa Salaroli for technical assistance. The authors also thank Manoela Ramalho, Mario Tyago Murakami, Simone Raposo Cotta, and Rodrigo Gouvêa Taketani for their constructive insights and suggestions. The research was funded by Fundação de Amparo à Pesquisa do Estado de São Paulo (FAPESP, grant #2019/03746-0). M.O.B. received PhD scholarships from FAPESP (# 2021/08013-0) and Coordenação de Aperfeiçoamento de Pessoal de Nível Superior - Brazil (CAPES) - Finance Code 001. A.R. received a research fellowship from Conselho Nacional de Desenvolvimento Científico e Tecnológico (CNPq, #305269/2018).

Author contributions

Mariana de Oliveira Barcoto - Conceptualization, Data curation, Formal analysis (metabarcoding data, SEM, and scoring), Investigation, Methodology, Project administration, Visualization, Writing – original draft, and Writing – review & editing. Raquel Lima de Sousa - Investigation (experiments and data collection), Methodology. João Gabriel da Silva Soares - Formal analysis (NMR data). Rodrigo Henrique dos Santos Garcia - Formal analysis (NMR data). Eduardo Ribeiro de Azevedo - Formal analysis (NMR data), Resources, Validation, Writing – review & editing. Lucas William Mendes - Formal analysis (metabarcoding data), Software, Resources, Writing – review & editing. Odair Correa Bueno - Resources, Writing – review & editing. Andre Rodrigues - Conceptualization, Methodology, Project administration, Supervision, Resources, Funding acquisition, Writing – review & editing.

Competing interests

The authors declare no competing interests.

Additional information

Supplementary information The online version contains supplementary material available at https://doi.org/10.1038/s41522-025-00876-7.

Correspondence and requests for materials should be addressed to Mariana de Oliveira Barcoto or Andre Rodrigues.